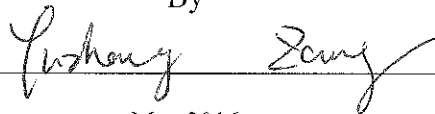


UWB Motion and Micro-Gesture Detection
–Applications to interactive electronic gaming and remote sensing

by
Yuzhang Zang

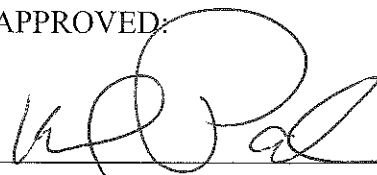
A Thesis
Submitted to the Faculty
of the
WORCESTER POLYTECHNIC INSTITUTE
In partial fulfillment of the requirements for the
Degree of Master of Science
in
Electrical and Computer Engineering

By

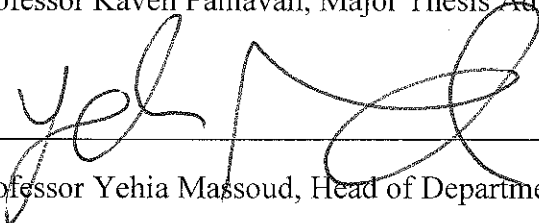


May 2016

APPROVED:



Professor Kaveh Pahlavan, Major Thesis Advisor



Professor Yehia Massoud, Head of Department

Abstract

The ultra-wideband (UWB) technology has a vast unlicensed frequency spectrum, which can support precise indoor positioning in orders of centimeters. The features of UWB signals can be utilized for variety of applications. In this project first we present an empirical channel models to analyze the localization accuracy of the UWB technology for interactive electronic gaming (Ping-Pong) in Line-of-Sight (LOS) and Obstructed LOS (OLOS) scenarios. Then we introduce a new concept, which we refer to as micro-gesture detection. Our micro-gesture detection concept uses features of UWB signal while one antenna is held by the user to handle the more refined motions of the hand such as rotation. We use four specific features of the UWB signals: time of arrival, power of the first peak, total power, and the Root-Mean Square (RMS) of the delay spread, for this purpose. As the hand rotates the position of the antenna in the hand and the external antenna changes from LOS to OLOS. We compare gesture detection using multiple features of the UWB signal with traditional gesture detection using the received signal strength (RSS) of the Wi-Fi signal. We foresee micro-gesture detection capabilities become helpful for the people with limited mobility or visually impaired for implementation of simplified sign languages to communication with electronic devices located away from the person.

Acknowledgements

First, I would like to express my deepest gratitude and respect to my advisor Kaveh Pahlavan, who guides me to the research field, who provides me the chance to take a glimpse of the world of engineering and who keeps sharing his sagacious tips on life and research. He is always generous on giving wise advises and helping me out when I encountered difficulties in my research. It is my honor to spend two years studying in CWINS Lab and to have him as my research advisor.

I am grateful to have Professor Lifeng Lai, Professor Agu Emmanuel to be my committee members. Thank you for the priceless comments and reviewing of this thesis. And I would like to express my special thankfulness to Mr. Yang Zheng, a former master student in CWINS Lab, for his constant help and leading during my first year of Master's study. Special thanks to Yishuang Geng and Bader Alkandari, for their patient guide and providing abundant resources for my research. I also would like to say thanks to former and current members in CWINS Lab. Thank you so much for offering me a friendly yet active atmosphere in the lab, which is like a big family.

Finally, I would like to say that I owe my family. I cannot finish my Master's study without the support and believe from my parents, they always stand on my side when I was frustrated or depressed, even though they know little about what I am doing exactly.

Contents

Abstract.....	I
Acknowledgements.....	II
Chapter 1 Introduction.....	1
1.1 Background and Motivation.....	1
1.2 Contribution of the thesis.....	3
1.3 Outline of the thesis Report.....	4
Chapter 2 Background in UWB Application.....	5
2.1 Motion Gaming.....	5
2.1.1 Motion Gaming Development.....	5
2.1.2 Nintendo Gaming Platform Wii.....	6
2.1.3 Microsoft Platform Kinect.....	11
2.2 Gesture Detection.....	14
2.2.1 Active gesture detection.....	16
2.2.2 Positive gesture detection.....	17
2.3 UWB Application and Behavior.....	19
2.3.1 Behavior of UWB Signal.....	21
2.3.2 Tools for Performance Evaluation of UWB System.....	23
Chapter 3 UWB Localization Modeling for Electronic Gaming.....	25
3.1 Measurement system and scenario.....	25
3.2 Error Classification.....	32
3.3 Modeling on Effect of Multipath.....	32
3.4 Modeling on Effect of Human Body.....	36
3.5 Modeling on Effect of Bandwidth.....	37

Chapter 4 Micro-Gesture Detection using UWB	45
4.1 Measurement System and scenario.....	46
4.1.1 Wi-Fi gesture detection.....	46
4.1.2 UWB gesture detection	49
4.2 Data analysis and results.....	53
Chapter 5 Summary, Conclusion and future work.....	60
Reference	62
Appendix A Original Data	70
Appendix B Core code.....	84

List of Figures

2.1 Nintendo Wii remote game controller	7
2.2 IR camera chip.....	8
2.3 A depiction of an accelerometer designed at Sandia National Laboratories	10
2.4 Diagram of a gyro wheel. Reaction arrows about the output axis (blue) correspond to forces applied about the input axis (green), and vice versa	11
2.5 Infrared projector, IR camera, and RGB camera inside a Kinect sensor	12
2.6 A CCD image sensor on a flexible circuit board	13
3.1 Agilent Network Analyzer used to collect and analyze data	26
3.2 Laser rangefinder to measure the real distance	27
3.3 Antenna attached to a Ping-Pong racket	27
3.4 Gaming gestures in Ping Pong used for modeling	28
3.5 Measurement scenario for interactive electronic Ping- Pong gaming (a)Picture of the whole system (b)Test area and locations on the table	30
3.6 Channel profiles of sample measurement in each location with picked peaks for interactive electronic Ping- Pong gaming	31
3.7 Measurement environment multipath model (a) measurement environment in the Lab (b) multipath pattern simulation in measurement scenario	33
3.8 PDF of distance measurement error in three different position 3, 6, 9	34
3.9 Multipath effect on variance, vertical axis is the variance of the distance measurement error and the horizontal axis represents the distance between transmitter and the receiver.....	35
3.10 Body Effect in Static Point Distance Measurement	36
3.11 Measurement of channel profile in 2 GHz (a) LOS condition (b) OLOS condition.....	37
3.12 Channel profile of two sample tests with operating bandwidth (a) 2GHz (b) 500MHz.....	38

3.13 Original relationship between mean & variance of error and operation bandwidth in LOS & OLOS conditions (a) Mean of error in LOS condition (b) Variance of error in LOS condition (c) Mean of error in OLOS condition (d)Variance of error in OLOS condition	40
3.14 Bandwidth effect on (a)mean and (b)variance of error in LOS condition	42
3.15 Bandwidth effect on (a)mean and (b)variance of error in OLOS condition.....	43
4.1 Gestures used to detected and results in WiSee	47
4.2 Measurement system for Using Wi-Fi signals	48
4.3 Application used in the smart phone to collect the RSS data	48
4.4 Router used to generate Wi-Fi signal	49
4.5 Measurement system for using UWB signals	51
4.6 The UWB directional antenna	51
4.7 Sample of the measurement in two gestures (a) Gesture 1(b) Gesture 2	52
4.8 Different hand gestures' RSS and spectrograms	54
4.9 Profile distrubitions of two different positions(a) Postion 1(b) Postion 2	55
4.10 Mean of τ_{rms} and received in LOS and OLOS	57
4.11 First peak power in LOS and OLOS scenarios	57
4.12 Total power in LOS and OLOS scenarios	58

List of Tables

Table 1 Mean & variance of the ranging error on the effect of operating bandwidth	39
Table 2 Original data of the distance between the two antennas	70

Chapter 1 Introduction

In this Chapter, we give the introduction of our report as well as the short introduction of UWB technology and its application. In the second part, we give the reason of why we choose UWB to do the localization and gesture detection. Moreover, the contribution and outline are also been shown.

1.1 Background and Motivation

With the exponential growth of the video gaming industry new challenges emerge. Motion gaming has become a standard feature in every gaming system. To enhance the user experience innovative localization and tracking techniques are introduced. These techniques have their trade-offs [1][2][3][4], for popular motion gaming applications such as table tennis, an accurate localization and fast motion tracking are needed. So we should find a new one that can apply into more games like tennis for two players, which need the accurate relative position as well as getting rid of the human body effect. Therefore, ultra-wideband (UWB) has been chosen

UWB technology has been recognized as an ideal candidate for providing positioning information in indoor environments, in which the traditional services provided by e.g. the GPS are usually not available, unreliable or inaccurate [5]. It offers a vast unlicensed frequency band, which also allows novel uncoordinated ways of access to spectrum resources. UWB is a new horizon for short distance localization within 3 meters, which is very applicable to motion gaming scenarios. By modeling a resource management problem as a game, some aspects of a real-world implementation have to be relaxed. For instance, the number of players in a game is conventionally assumed constant but in real networks it changes over time. Furthermore, the available computing power of wireless sensor nodes is

limited because of energy and simple hardware constraints. Hence, games require utility functions with low complexity.

Besides, as computing moves increasingly away from the desktop, there is a growing need for new ways to interact with computer interfaces. Gestures enable a whole new set of interaction techniques for always-available computing embedded in the environment. For example, using a swipe hand motion in-air, a user could control the music volume while showering, or change the song playing on a music system installed in the living room while cooking, or turn up the thermostat while in bed. Such a capability can enable applications in diverse domains including home-automation, elderly health care, and gaming. However, the burden of installation and cost make most vision-based sensing devices hard to deploy at scale, for example, throughout an entire home or building. Given these limitations, researchers have explored ways to move some of the sensing onto the body and reduce the need for environmental sensors. However, even on-body approaches are limited to what people are willing to constantly carry or wear, and may be infeasible in many scenarios

RSS based gesture detection using Wi-Fi signal has attracted considerable attentions. UWB technology offers more features for gesture detection in indoor environments, which can be applied to medical applications to enhance its accuracy, agility and functionality.

The most frequently used distance measurement method for accurate indoor positioning is time-of-arrival (TOA) estimation of the direct path (DP) using ultra-wideband (UWB) technology [6] [7] [8]. Due to severe multipath conditions in indoor areas, estimation of TOA of DP results in small random and sometimes large errors. Paths arriving close to the detected first path cause the small random errors. The large errors occur when the DP goes below the detection threshold so

the detected first path in the received multipath profile is erroneously considered to be the DP. We refer to these situations as undetected direct path (UDP) conditions [9] [10].

By using UWB, we can confer some problems in using other technologies such as: Camera technologies have overlapping problems for multi-players; Battery operated devices may lose their maximum transmitted power in time; Shadow fading is a function of distance and it is negligible when we are close to the transmitter. So UWB is the most suitable technology for localization and gesture detection.

1.2 Contribution of the thesis

In this project first we present an empirical channel models to analyze the localization accuracy in interactive electronic ping pong gaming using UWB signals in Line-of-Sight (LOS) and Obstructed LOS (OLOS) scenarios and demonstrated that some features of UWB signal can be used for motion and gesture detection. These results are presented in the paper:

Yang Zheng, **Yuzhang Zang** and Kaveh Pahlavan, “UWB Localization Modeling for Electronic Gaming”, IEEE International Conference on Consumer Electronics (ICCE), Las Vegas, USA, January 9-12, 2016.

Secondly, we introduce a method for gesture detection using four features of the UWB signals (time of arrival, first peak power, total power and the Root-mean Square (RMS) delay spread) applied to remote sensing for the limited ability or visually impaired patients. We finally compare gesture detection using multiple

features of the UWB signal with traditional gesture detection using the received signal strength (RSS) of the Wi-Fi signal. The results are presented in the paper:

Yuzhang Zang, Kaveh Pahlavan, Yang Zheng and Le Wang, “UWB Gesture Detection for Visually Impaired Remote Control”, IEEE International Symposium on Medical Information and Communication Technology (ISMICT), Worcester, USA, March 21-23, 2016.

1.3 Outline of the thesis Report

This report is organized as follows: In chapter 2, we introduce the background of motion gaming and gesture detection. Besides, we show the details of UWB behavior and technical tools for the research. Chapter 3 describes the UWB localization modeling for electronic gaming, which includes the measurement system and scenario, the data analysis and results. In Chapter 4, we give all the details of micro-gesture detection using UWB technologies and the compare with RSS based gesture detection. Then, we show our conclusions and future work in Chapter5.

Chapter 2 Background in UWB Application

In this chapter, in the first part, we describe the development of motion gaming industry, which has two platforms, Wii and Kinect. And then we give the details of this two things and what kinds of technologies are applied to them. In the second part, we introduce the concept of gesture detection and its classification. Finally, we introduce the UWB application and its behavior.

2.1 Motion Gaming

In this section, we give a full introduction of the motion gaming, including its development and two platforms: Wii and Kinect. We also introduce the technologies and equipment used in the platforms: accelerometer, gyroscope as well as the image-sensing camera.

2.1.1 Motion Gaming Development

Motion sensing game is a new type of electronic games with the body to feel. Electronic game breaks the mode of operation in the past simply to handle key input, but to operate through changes in body movements.

The Wii is a home video game console released by Nintendo on November 19, 2006. As a seventh-generation console, the Wii competes with Microsoft's Xbox 360 and Sony's PlayStation 3. Nintendo states that its console targets a broader demographic than that of the two others.

Kinect is a line of motion sensing input devices by Microsoft for Xbox 360 and Xbox One video game consoles and Windows PCs. Based around a webcam-style add-on peripheral, it enables users to control and interact with their

console/computer without the need for a game controller, through a natural user interface using gestures and spoken commands.

2.1.2 Nintendo Gaming Platform Wii

The Wii Remote (shown in Figure 2.1) is the primary controller for the console. It uses a combination of built-in accelerometers and infrared detection to sense its position in 3D space when pointed at the LEDs in the Sensor Bar. This design allows users to control the game with physical gestures as well as button-presses.

The device bundled with the Wii retail package is the Nunchuk unit, which features an accelerometer and a traditional analog stick with two trigger buttons. In addition, an attachable wrist strap can be used to prevent the player from unintentionally dropping (or throwing) the Wii Remote. Nintendo has since offered a stronger strap and the Wii Remote Jacket to provide extra grip and protection. The Wii MotionPlus is another accessory that connects to the Wii Remote to supplement the accelerometer and sensor-bar capabilities, enabling actions to appear on the screen in real time. Further augmenting the remote's capabilities is the Wii Vitality Sensor, a fingertip pulse oximeter sensor that connects through the Wii Remote.

Work has been done in this area, of which the most widely known is by Johnny Chung Lee at Carnegie Mellon University [12]. His project demonstrates the use of two infrared sources and a Wii Remote [13] to track his head behind a computer screen. The application is created with the use of Direct X and the Microsoft Windows operating system. We designed native head tracking methods in Windows with the use of Windows based OpenGL and made it as a library which can be used in any OpenGL application. Furthermore we have used the library to develop an application for image manipulations.

And the latest one presenting a novel OpenGL based method to interact with the computer using Wii Remote device. We implemented two techniques i.e. Head Tracking and Image Viewer with touch screen capability. In the head-tracking phase we described how the data returned from the IR camera (shown in Figure 2.2) could be used to navigate in a 3D world. The application can be used for example in video games or even in scientific visualization. The user will be able to control a part of what he/she sees in his application by moving his head.

In the Image viewer we have shown an intuitive method for viewing images displayed on the monitor using only hand gestures. The image can be manipulated corresponding to the movement of the hands of the user including the Touch Screen feature.



Fig.2.1 Nintendo Wii remote game controller [11]



Fig.2.2 IR camera chip .Integrated multi-object tracking minimizes wireless data transmission

[14]

An accelerometer is a device that measures proper acceleration (shown in Fig 2.3). Proper acceleration is not the same as coordinate acceleration. For example, an accelerometer at rest on the surface of the Earth will measure an acceleration $g=9.81 \text{ m/s}^2$ straight upwards. By contrast, accelerometers in free fall orbiting and accelerating due to the gravity of Earth will measure zero.

Accelerometers have multiple applications in industry and science. Highly sensitive accelerometers are components of inertial navigation systems for aircraft and missiles. Accelerometers are used to detect and monitor vibration in rotating machinery. Accelerometers are used in tablet computers and digital cameras so that images on screens are always displayed upright. Accelerometers are used in drones for flight stabilization. Pairs of accelerometers extended over a region of space can be used to detect differences (gradients) in the proper accelerations of frames of references associated with those points. These devices are called gravity

gradiometers, as they measure gradients in the gravitational field. Such pairs of accelerometers in theory may also be able to detect gravitational waves.

Single and multi-axis models of accelerometer are available to detect magnitude and direction of the proper acceleration (or g-force), as a vector quantity, and can be used to sense orientation (because direction of weight changes), coordinate acceleration (so long as it produces g-force or a change in g-force), vibration, shock, and falling in a resistive medium (a case where the proper acceleration changes, since it starts at zero, then increases). Micro-machined accelerometers are increasingly present in portable electronic devices and video game controllers, to detect the position of the device or provide for game input.

A gyroscope is a device for measuring or maintaining orientation, based on the principle of preserving angular momentum. Mechanical gyroscopes typically comprise a spinning wheel or disc in which the axle is free to assume any orientation. Although the orientation of the spin axis changes in response to an external torque, the amount of change and the direction of the change is less and in a different direction than it would be if the disk were not spinning. When mounted in a gimbal (which minimizes external torque), the orientation of the spin axis remains nearly fixed, regardless of the mounting platform's motion.

Gyroscopes based on other operating principles also exist, such as the electronic, microchip-packaged MEMS gyroscope devices found in consumer electronic devices, solid-state ring lasers, fibre optic gyroscopes, and the extremely sensitive quantum gyroscope.(shown in Fig 2.4)

Applications of gyroscopes include inertial navigation systems where magnetic compasses would not work (as in the Hubble telescope) or would not be precise enough (as in intercontinental ballistic missiles), or for the stabilization of flying

vehicles like radio-controlled helicopters or unmanned aerial vehicles, and recreational boats and commercial ships. Due to their precision, gyroscopes are also used in gyrotheodolites to maintain direction in tunnel mining. Gyroscopes can be used to construct gyrocompasses, which complement or replace magnetic compasses (in ships, aircraft and spacecraft, vehicles in general), to assist in stability (Hubble Space Telescope, bicycles, motorcycles, and ships) or be used as part of an inertial guidance system.

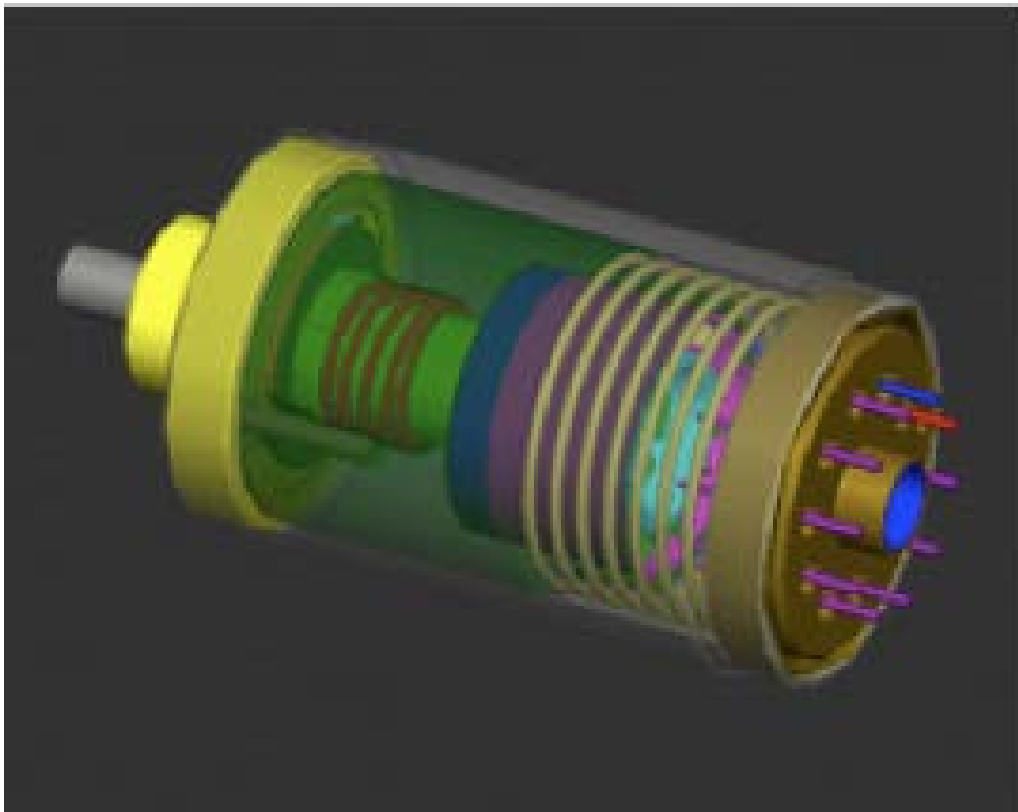


Fig.2.3 A depiction of an accelerometer designed at Sandia National Laboratories[15]

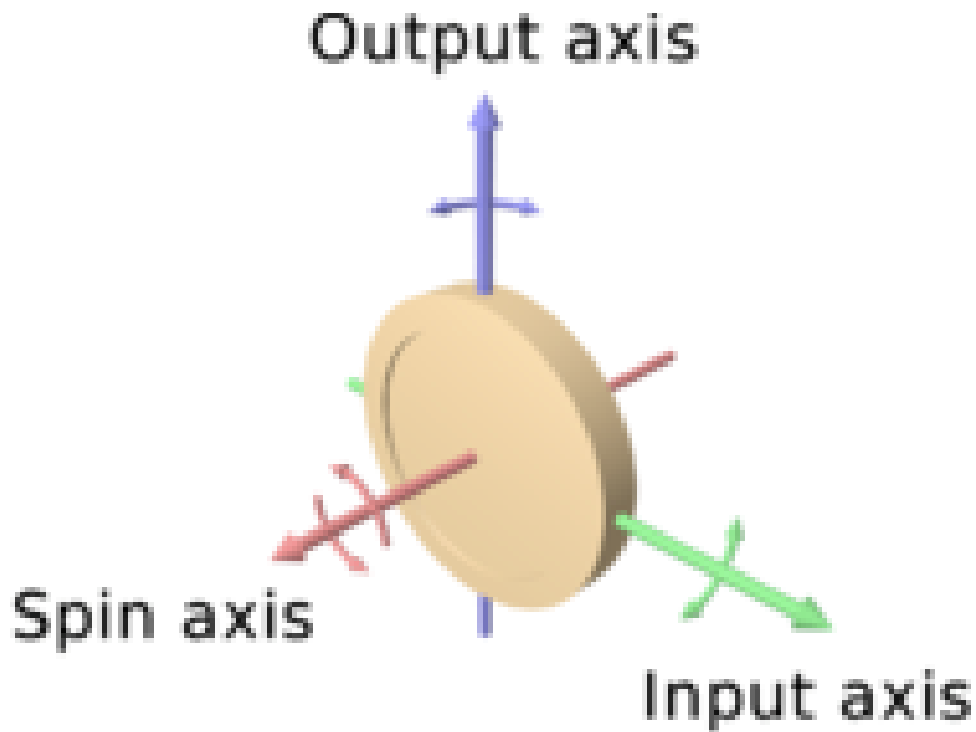


Fig.2.4 Diagram of a gyro wheel. Reaction arrows about the output axis (blue) correspond to forces applied about the input axis (green), and vice versa. [16]

2.1.3 Microsoft Platform Kinect

Kinect builds on software technology developed internally by Rare, a subsidiary of Microsoft Game Studios owned by Microsoft, and on range camera technology by Israeli developer Prime Sense, which developed a system that can interpret specific gestures, making completely hands-free control of electronic devices possible by using an infrared projector and camera and a special microchip to track the movement of objects and individuals in three dimensions.

Kinect sensor (shown in Figure 2.5) is a horizontal bar connected to a small base with a motorized pivot and is designed to be positioned lengthwise above or below the video display. The device features an RGB camera, depth sensor and

multi-array microphone running proprietary software", which provide full-body 3D motion capture, facial recognition and voice recognition capabilities. The depth sensor consists of an infrared laser projector combined with a monochrome CMOS sensor, which captures video data in 3D under any ambient light conditions. The sensing range of the depth sensor is adjustable, and Kinect software is capable of automatically calibrating the sensor based on gameplay and the player's physical environment, accommodating for the presence of furniture or other obstacles.

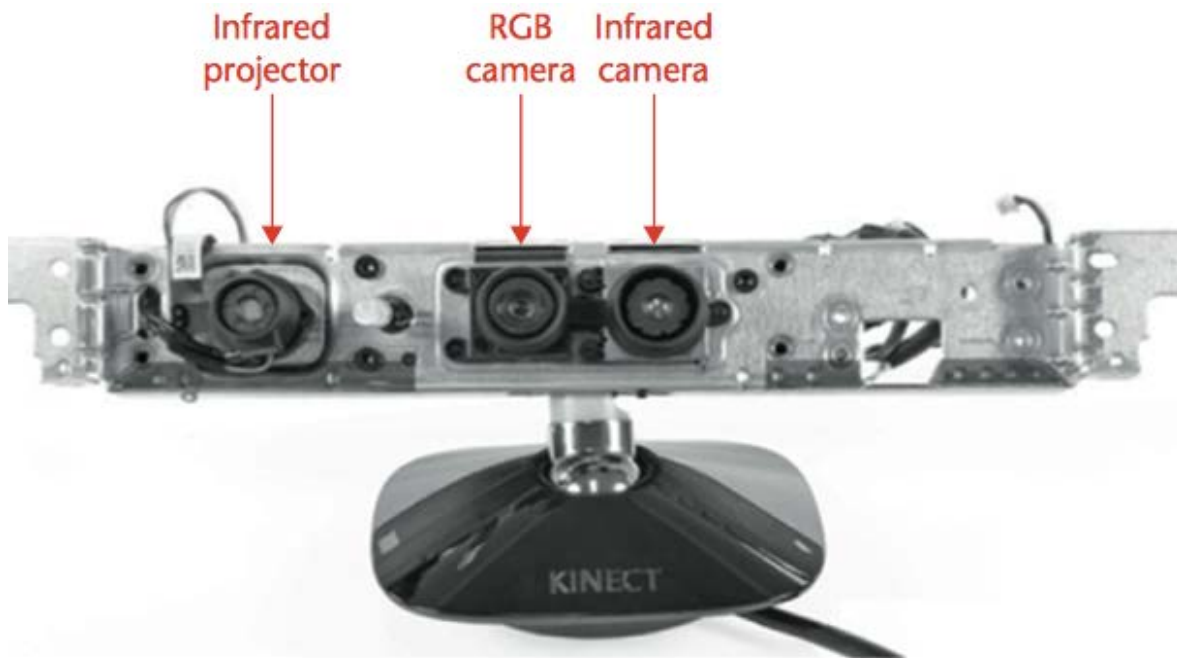


Fig.2.5 Infrared projector, IR camera, and RGB camera inside a Kinect sensor [17]

An image sensor or imaging sensor is a sensor that detects and conveys the information that constitutes an image. It does so by converting the variable attenuation of waves (as they pass through or reflect off objects) into signals, the small bursts of current that convey the information. The waves can be light or other electromagnetic radiation. Image sensors are used in electronic imaging devices of both analog and digital types, which include digital cameras, camera modules,

medical imaging equipment, night vision equipment such as thermal imaging devices, radar, sonar, and others. As technology changes, digital imaging tends to replace analog imaging.

Early analog sensors for visible light were video camera tubes; currently used types are semiconductor charge-coupled devices (CCD) or active pixel sensors in complementary metal-oxide-semiconductor (CMOS) or N-type metal-oxide-semiconductor (NMOS, Live MOS) technologies. Analog sensors for invisible radiation tend to involve vacuum tubes of various kinds; digital sensors include flat panel detectors.

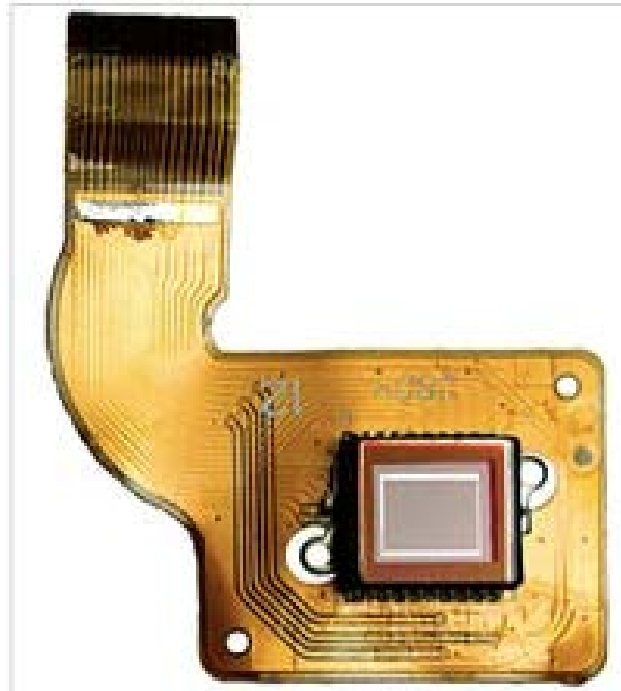


Fig.2.6 A CCD image sensor on a flexible circuit board[18]

2.2 Gesture Detection

Gestures can be used to control the distribution of resources in hospitals, interact with medical instrumentation, control visualization displays and help handicapped users as part of their rehabilitation therapy. [19][20][21]

We humans use gestures to interact with our environment during the earliest stages of our development. We also communicate using such gestures as body movement, facial expression, and finger pointing. Though much has been written about gesture interfaces, interface technology rarely adopts this media; consequently, expressiveness and naturalness elements are missing from most user interfaces. Hand-gesture applications provide three main advantages over conventional human-machine interaction systems: Accessing information while maintaining total sterility. Touchless interfaces are especially useful in healthcare environments; Overcoming physical handicaps. Control of home devices and appliances for people with physical handicaps and/or elderly users with impaired mobility; and exploring big data. Exploration of large complex data volumes and manipulation of high-quality images through intuitive actions benefit from 3D interaction, rather than constrained traditional 2D methods. [22]

Some of these concepts have been exploited to improve medical procedures and systems, like the automotive field and the medical sector. The first application of hand-gesture control we review—medical systems and assistive

technologies—provides the user sterility needed to help avoid the spread of infection. As a result, gesture detection systems are becoming increasingly competitive in some special application areas.

Graetzel [23] covered ways to incorporate hand gestures into doctor-computer interfaces, describing a computer-vision system that enables surgeons to perform standard mouse functions, including pointer movement and button presses, with hand gestures that satisfy the “intuitiveness” requirement. A European Community Project called WearIT [24] satisfies the “comfort” requirement by encouraging physicians to use a wrist-mounted RFID reader to identify the patient and interact through gestures with the hospital information system to document exams and write prescriptions, helping ensure sterility. For the impaired, the critical requirements of a hand-gesture interface system are “user adaptability and feedback” and “come as you are.” In this context, wheelchairs, as mobility aids, have been enhanced through robotic/ intelligent vehicles able to recognize hand-gesture commands (such as in Kuno [25]). The Gesture Pendant [26] is a wearable gesture-recognition system used to control home devices and provide additional functionality as a medical diagnostic tool. The Staying Alive [27] virtual-reality-imagery-and-relaxation tool satisfies the “user adaptability and feedback” requirement, allowing cancer patients to navigate through a virtual scene using [28] traditional T'ai Chi gestures. In the same vein, a tele-rehabilitation

system [29] for kinesthetic therapy—treatment of patients with arm-motion coordination disorders— uses force-feedback of patient gestures. Force-feedback was also used by Patel and Roy [30] to guide an attachable interface for individuals with severely dysarthria speech. Also, a hand-worn haptic glove was used to help rehabilitate post-stroke patients in the chronic phase by Boian. [31]

These systems illustrate how medical systems and rehabilitative procedures promise to provide a rich environment for the potential exploitation of hand-gesture systems. [32][33]

Gestures enable a whole new set of interaction technologies for always-available computing embedded in the environment. For example, with the sensor attached to the hand, visually impaired people can control the volume of the radio and change the channel.

2.2.1 Active gesture detection

To recognize human activities, physical sensors (camera, accelerometer, gyroscope, etc.) are often deployed in environments, attached on objects or worn on human bodies to continuously collect sensor readings. Then, based on predefined pattern recognition models, the activity types are identified at an aggregator for upper layer applications. These sensor-based methods are called traditional activity recognition methods. They can be roughly divided into three

categories: (1) wearable motion sensor based methods [34], which utilize on-body motion sensors (accelerometer, gyroscope, etc.) to sense the movements of body parts, such as [35-43]; (2) camera sensor based methods [44], which take advantage of camera to record the video sequence and recognize the activities using computer vision algorithms. According to the camera type, the video may be RGB video (e.g. [45, 46]), depth video (e.g. [47, 48]) or RGB-D video (e.g. [49,50]); (3) environmental variable based methods, which use physical sensors (pressure, proximity, RFID, etc.) to infer human activities from the status of used objects or change of environmental variables, such as [51-53]. Although traditional activity recognition methods obtain good performances and are widely accepted, they require specific sensing modules and raise some concerns such as privacy, energy consumption and deployment cost.

2.2.2 Positive gesture detection

The passive approach compared with traditional activity recognition methods, radio based methods utilize wireless transceivers in environments as infrastructure, exploit radio communication characters to achieve high recognition accuracy, reduce energy cost and preserve users' privacy. We divide radio-based methods into four categories: Zig-Bee [54] radio based activity recognition, Wi-Fi [55] radio based activity recognition, RFID radio [56] based activity recognition, and other radio based activity recognition. [57][58] Zig-Bee is a low-cost, low-power,

wireless mesh network standard [59]. It is widely used in wireless sensor network, e.g. body sensor network [60–64] Compared with Zig-Bee radio based activity recognition, Wi-Fi radio based activity recognition can take advantage of existing Wi-Fi infrastructure in an office building, shopping mall, etc. [65-71]

Two kinds of RF signals will be introduced in this part. The first one is narrow-band signal using RSS (received signal strength) as a parameter to analyze; the second one is the wide-band signal using ultra wide-band (UWB) features.

Received signal strength indicator is a measurement of the power present in a received radio signal. Theoretically, the RSSI should be stayed in the one value. RSS measurement is a packet-level estimator and represents the signal power over a packet as single amplitude. With the collected amplitude information, the structure of magnitude changes and the timing information are combined to classify different gestures. However, due to the multi-path reflection, diffraction and shadow fading, the RSSI varies a lot. Especially when some gestures are made between the transmitter and receiver, RSSI fluctuates more. [72][73]

UWB technology has been recognized as an ideal candidate for gesture detection in indoor environments, in which the traditional services are usually not available, unreliable or inaccurate. It offers a vast unlicensed frequency band, which also allows novel uncoordinated ways of access to spectrum resources. By

using UWB signal, we can have more parameters to do the analysis, such as time of arrival (TOA), first peak power, total power and the RMS delay spread.

2.3 UWB Application and Behavior

UWB technology has been recognized as an ideal candidate for providing positioning information in indoor environments, in which the traditional services provided by e.g. the GPS are usually not available, unreliable or inaccurate. It offers a vast unlicensed frequency band, which also allows novel uncoordinated ways of access to spectrum resources.

UWB is a new horizon for short distance localization within 3 meters, which is very applicable to motion gaming scenarios. By modeling a resource management problem as a game, some aspects of a real-world implementation have to be relaxed. For instance, the number of players in a game is conventionally assumed constant but in real networks it changes over time. Furthermore, the available computing power of wireless sensor nodes is limited because of energy and simple hardware constraints. Hence, games require utility functions with low complexity.

Impulse Radio (IR)-UWB radio technology, particularly in its low power, low data rate flavor, is a key technology for indoor joint communication and localization applications. Especially in industrial environments, e.g. production logistics, industrial automation or security applications, such systems will allow for many substantial process improvements. IR-UWB radio technology offers a vast

unlicensed frequency band, which also allows novel uncoordinated ways of access to spectrum resources.

IR-UWB technology allows multiple concurrent transmissions; hence, IR-UWB systems are subject to impulsive non-Gaussian interference [74]. Since interference is allowed to exist, some form of adaptability is required to manage it. Interference management is a cross-layer issue involving the physical layer and the link layer. On the link layer, techniques for controlling transmission parameters, e.g. the processing gain, the modulation order or the channel coding rate, have been subject of research [75-77]. In [78] a novel pulse repetition frequency (PRF) allocation scheme was introduced, which controls the channel access rate (in terms of pulses per second) of independent users in response to the perceived interference environment. Following a classical game theoretical formulation [79], this scheme combines the goal of maximizing the cumulative network throughput with user-centric QoS constraints. Results obtained by simulation showed that, based on link quality awareness, our PRF allocation approach is able to optimally configure the structure of IR-UWB signals to the level of interference experienced at the receiver. The principal drawback of this scheme is the high complexity of its utility function, which is contrary to the scarce computing resources available in wireless sensor nodes. In addition, further simulations have shown that a

time-varying number of players in the game, as it is expected under real working conditions, impair the quality of the results.

2.3.1 Behavior of UWB Signal

Time of arrival (TOA), sometimes called time of flight (TOF), is the travel time of a radio signal from a single transmitter to a remote single receiver. By the relation between light speed in vacuum and the carrier frequency of a signal the time is a measure for the distance between transmitter and receiver. However, in some publications the fact is ignored that this relation is well defined for vacuum, but is different for all other material when radio waves pass through.

Line-of-sight propagation is a characteristic of electromagnetic radiation or acoustic wave propagation. Electromagnetic transmission includes light emissions traveling in a straight line. The rays or waves may be diffracted, refracted, reflected, or absorbed by atmosphere and obstructions with material and generally cannot travel over the horizon or behind obstacles.

Non-line-of-sight (NLOS) or near-line-of-sight is radio transmission across a path that is partially obstructed, usually by a physical object in the innermost Fresnel zone. Many types of radio transmissions depend, to varying degrees, on line of sight (LOS) between the transmitter and receiver. Obstacles that commonly cause NLOS conditions include buildings, trees, hills, mountains, and, in some cases, high voltage electric power lines. Some of these obstructions reflect certain

radio frequencies, while some simply absorb or garble the signals; but, in either case, they limit the use of many types of radio transmissions, especially when low on power budget.

A body area network (BAN), also referred to as a wireless body area network (WBAN) or a body sensor network (BSN), is a wireless network of wearable computing devices. [80] BAN devices may be embedded inside the body, implants, may be surface-mounted on the body in a fixed position Wearable technology or may be accompanied devices, which humans can carry in different positions, in clothes pockets, by hand or in various bags. [81] Whilst, there is a trend towards the miniaturization of devices, in particular, networks consisting of several miniaturized body sensor units (BSUs) together with a single body central unit (BCU).

In wireless communications, fading is deviation of the attenuation affecting a signal over certain propagation media. The fading may vary with time, geographical position or radio frequency, and is often modeled as a random process. A fading channel is a communication channel that experiences fading. In wireless systems, fading may either due to multipath propagation, referred to as multipath induced fading, or due to shadowing from obstacles affecting the wave propagation, sometimes referred to as shadow fading.

Multipath is the propagation phenomenon that results in radio signals reaching the receiving antenna by two or more paths. Causes of multipath include atmospheric ducting, ionosphere reflection and refraction, and reflection from water bodies and terrestrial objects such as mountains and buildings.

Root mean square (abbreviated RMS or rms), also known as the quadratic mean in statistics is a statistical measure defined as the square root of the mean of the squares of a sample. In physics it is a value characteristic of a continuously varying quantity, such as a cyclically alternating electric current, obtained by taking the mean of the squares of the instantaneous values during a cycle. This is the effective value in the sense of the value of the direct current that would produce the same power dissipation in a resistive load. An electric current of given magnitude produces the same heating regardless of the direction of current flow; squaring the quantity measured ensures that alternation of sign does not invalidate the result. It can be calculated for a sequence of discrete values, or for a continuously varying function. The name is simply a description: the square root of the arithmetic mean of the squares of the samples. It is a particular case of the generalized mean, with exponent 2.

2.3.2 Tools for Performance Evaluation of UWB System

A network analyzer is an instrument that measures the network parameters of electrical networks. Today, network analyzers commonly measure s-parameters

because reflection and transmission of electrical networks are easy to measure at high frequencies, but there are other network parameter sets such as y-parameters, z-parameters, and h-parameters. Network analyzers are often used to characterize two-port networks such as amplifiers and filters, but they can be used on networks with an arbitrary number of ports.

A laser rangefinder is a rangefinder, which uses a laser beam to determine the distance to an object. The most common form of laser rangefinder operates on the time of flight principle by sending a laser pulse in a narrow beam towards the object and measuring the time taken by the pulse to be reflected off the target and returned to the sender. Due to the high speed of light, this technique is not appropriate for high precision sub-millimeter measurements, where triangulation and other techniques are often used.

MATLAB (matrix laboratory) is a multi-paradigm numerical computing environment and fourth-generation programming language. Developed by MathWorks, MATLAB allows matrix manipulations, plotting of functions and data, implementation of algorithms, creation of user interfaces, and interfacing with programs written in other languages, including C, C++, Java, Fortran and Python.

Chapter 3 UWB Localization Modeling for Electronic Gaming

In this chapter, we use UWB to do the localization for electronic gaming system. In the first section, we present the measurement system and scenario. In the next parts, we analysis the collected data and do the error modeling on the effect of multipath, human body and operating bandwidth.

3.1 Measurement system and scenario

In this section, we show both the measurement system and the scenario. In the system part, we introduce the network analyzer, the laser rangefinder as well as the antenna. In the scenario part, we introduce the background of table tennis, two conditions and locations in the scenario.

3.1.1 Measurement system

A network analyzer (shown in Figure 3.1) is an instrument that measures the network parameters of electrical networks. Today, network analyzers commonly measure s -parameters because reflection and transmission of electrical networks are easy to measure at high frequencies, but there are other network parameter sets such as y -parameters, z -parameters, and h -parameters. Network analyzers are often used to characterize two-port networks such as amplifiers and filters, but they can be used on networks with an arbitrary number of ports.



Fig.3.1 Agilent Network Analyzer used to collect and analyze data

A laser rangefinder (shown in Figure 3.2) is a rangefinder, which uses a laser beam to determine the distance to an object. The most common form of laser rangefinder operates on the time of flight principle by sending a laser pulse in a narrow beam towards the object and measuring the time taken by the pulse to be reflected off the target and returned to the sender. Due to the high speed of light, this technique is not appropriate for high precision sub-millimeter measurements, where triangulation and other techniques are often used.

We use a directional antenna in this experiment which works in the UWB form 3 to 8GHz, we attach the antenna to a table tennis racket (shown in Figure 3.3).

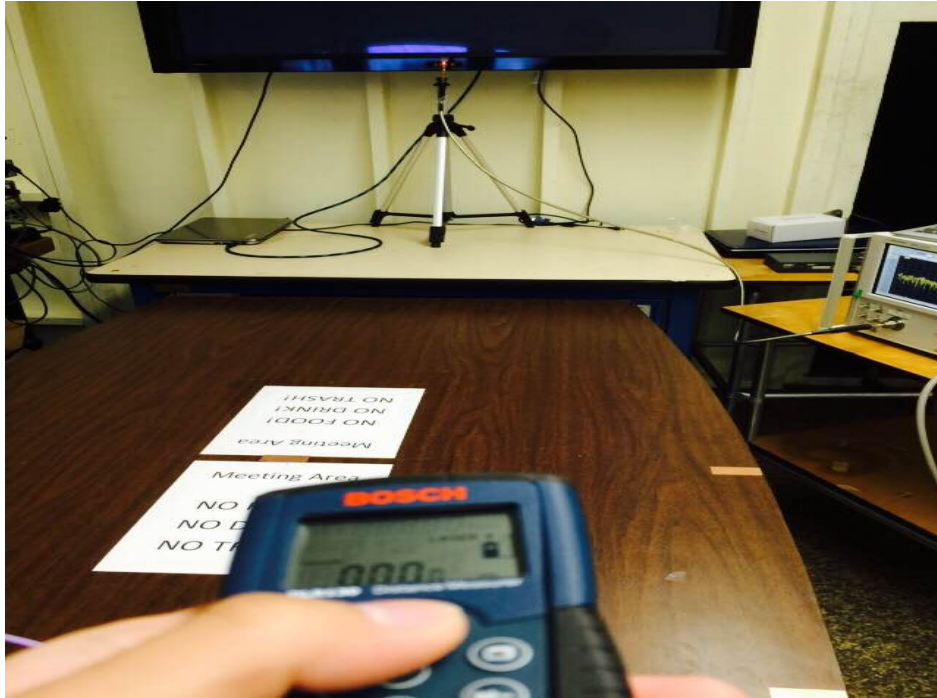


Fig.3.2 Laser rangefinder to measure the real distance

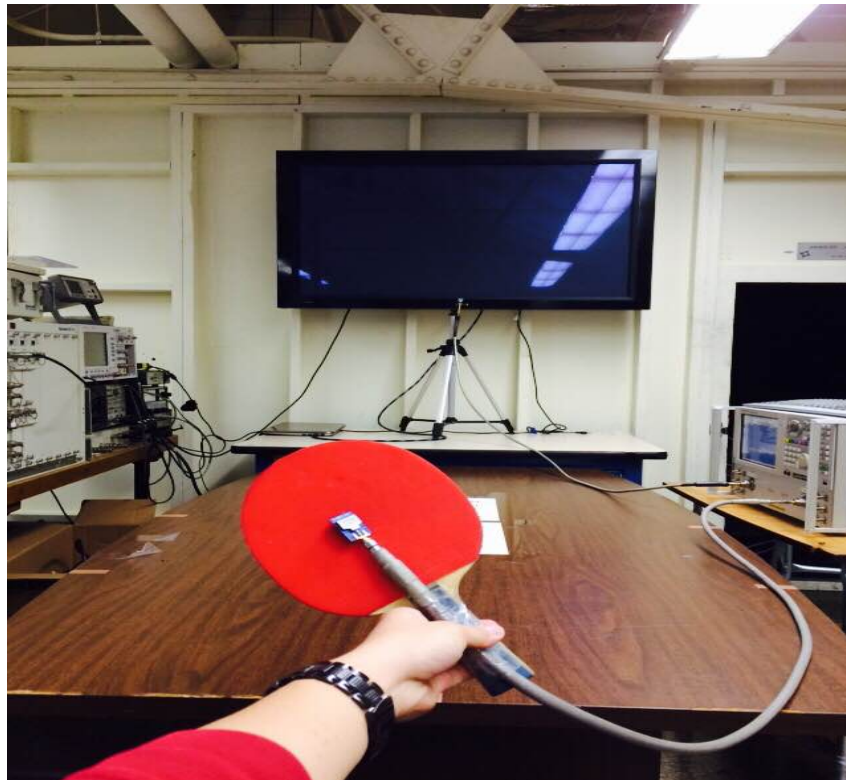


Fig.3.3 Antenna attached to a Ping-Pang racket

3.1.2 Measurement scenario

Traditional table tennis is an indoor sport, and since its inception of motion gaming is mainly used in indoor environments. For this reason, table tennis is one of the games that stand to gain the most from accurate space location and fast reaction. And also it has different kinds of gesture and locations (shown in Figure 3.4). So we choose it as a better choice for analysis and research in our scenario. To make the scenario more reasonable, we set it in a complicated indoor environment to simulate the real gaming scene.

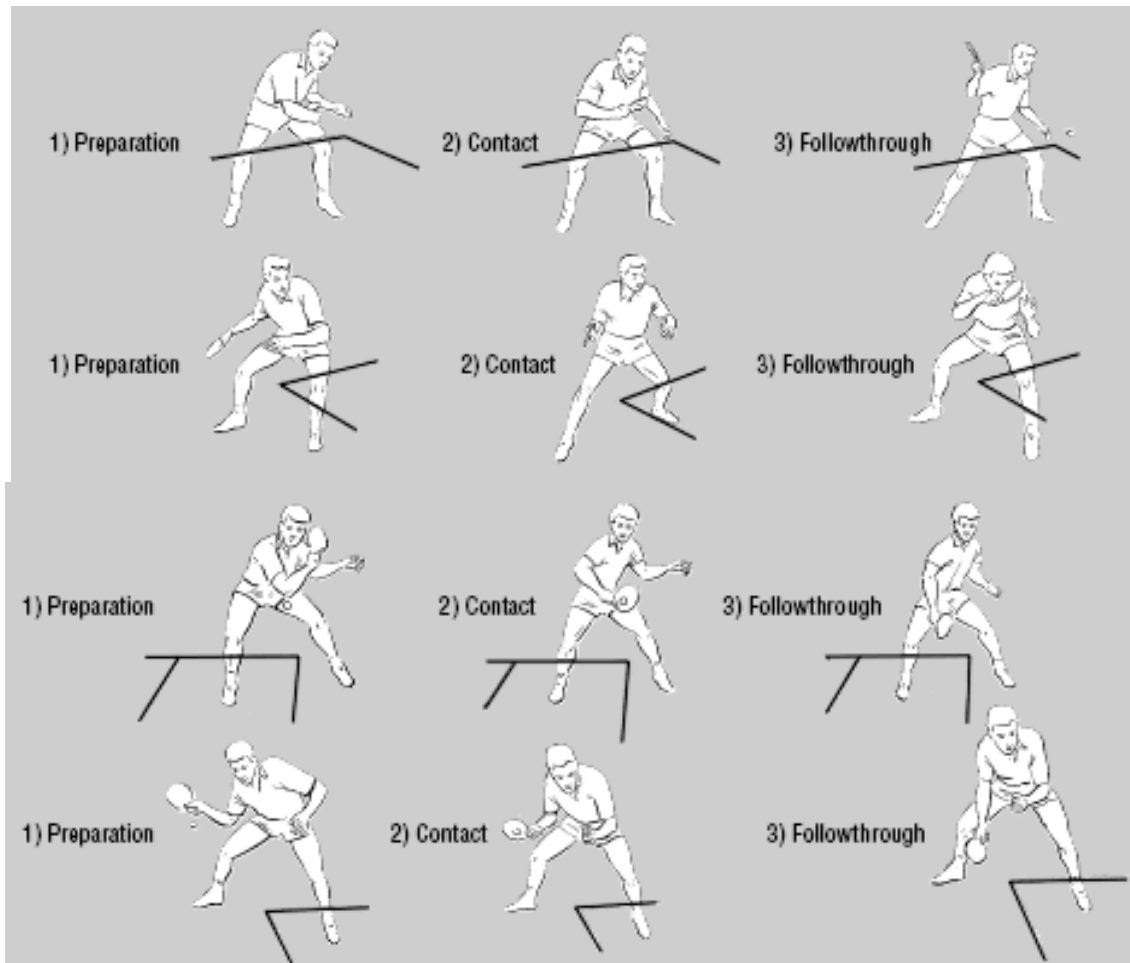
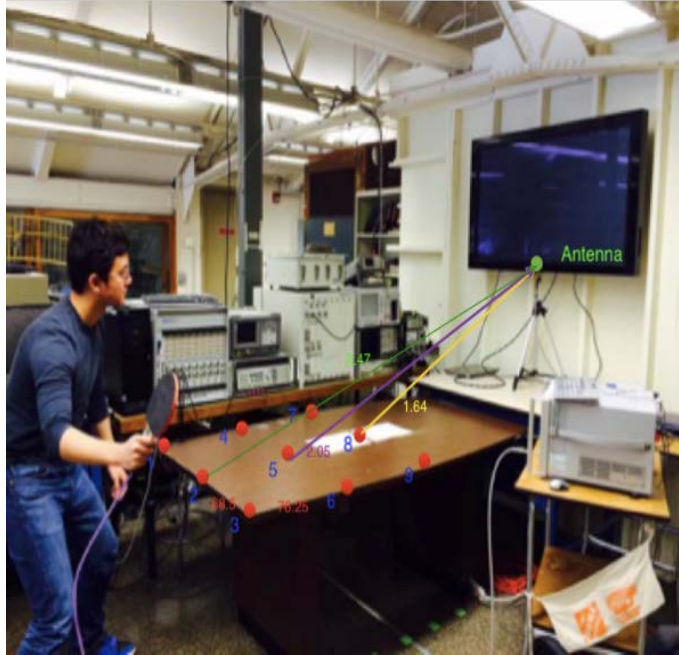


Fig.3.4 Gaming gestures in Ping Pong used for modeling

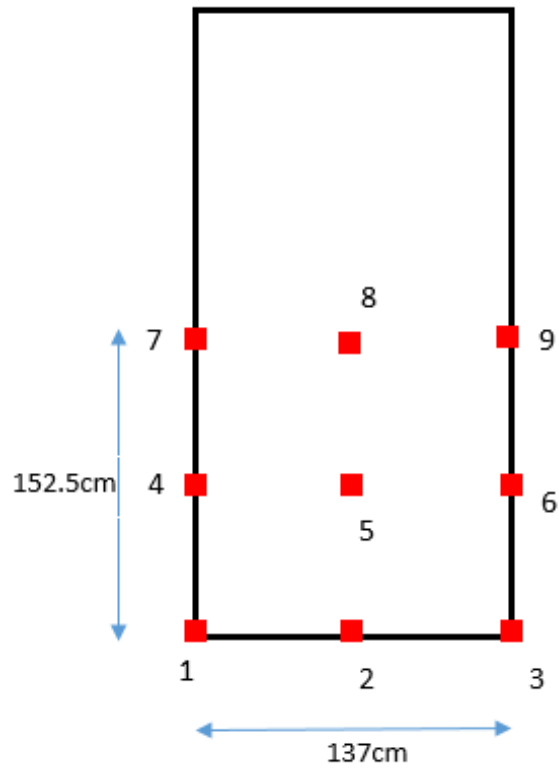
Two possible scenarios have been introduced in our measurement. The first one is LOS condition where the receiving antenna on the motion controller has a

direct line of site to the transmitter on the television. The second case is the OLOS condition where the user's hand covers or obstructs the LOS case due to the controller motion. We measure the Time-of-Arrival (TOA) using UWB antenna, one is on the television display, and another is on the motion controller in the user's hand. Besides, we use a digital laser tape to measure the real distance. Then repeat the measurement 500 times to measure and calculate the error of TOA for each location. During the measurement process, we change the bandwidth from 100MHz to 2.5GHz to analyze the effect of bandwidth in localization error and the error's variance of indoor gaming localization.

To measure the behavior of target node and base stations, a vector network analyzer has been employed in our measurement system. The measurements were carried out in the Atwater Kent Laboratory of Worcester Polytechnic Institute, using two UWB directional antennas, which have been connected to both transmit and receive port of the network analyzer through low loss RF cables. Moreover, a power amplifier has been added at the transmitter (TX) port of network analyzer to achieve better signal to noise ratio (SNR) at the receiver (RX) side. The vary frequency of operation of the network analyzer from 3 GHz to 8GHz. We choose 9 locations for measurement that are in the area of a 1.525m *1.370m rectangular. Fig. 3.5 show the measurement system and the testing points in the grid region. And in Fig. 3.6, we give the samples of measurement in each location. It shows the time of arrival and the power of each profile.



(a)



(b)

Fig.3.5 Measurement scenario for interactive electronic Ping- Pong gaming(a)Picture of the whole system (b)Test area and locations on the table

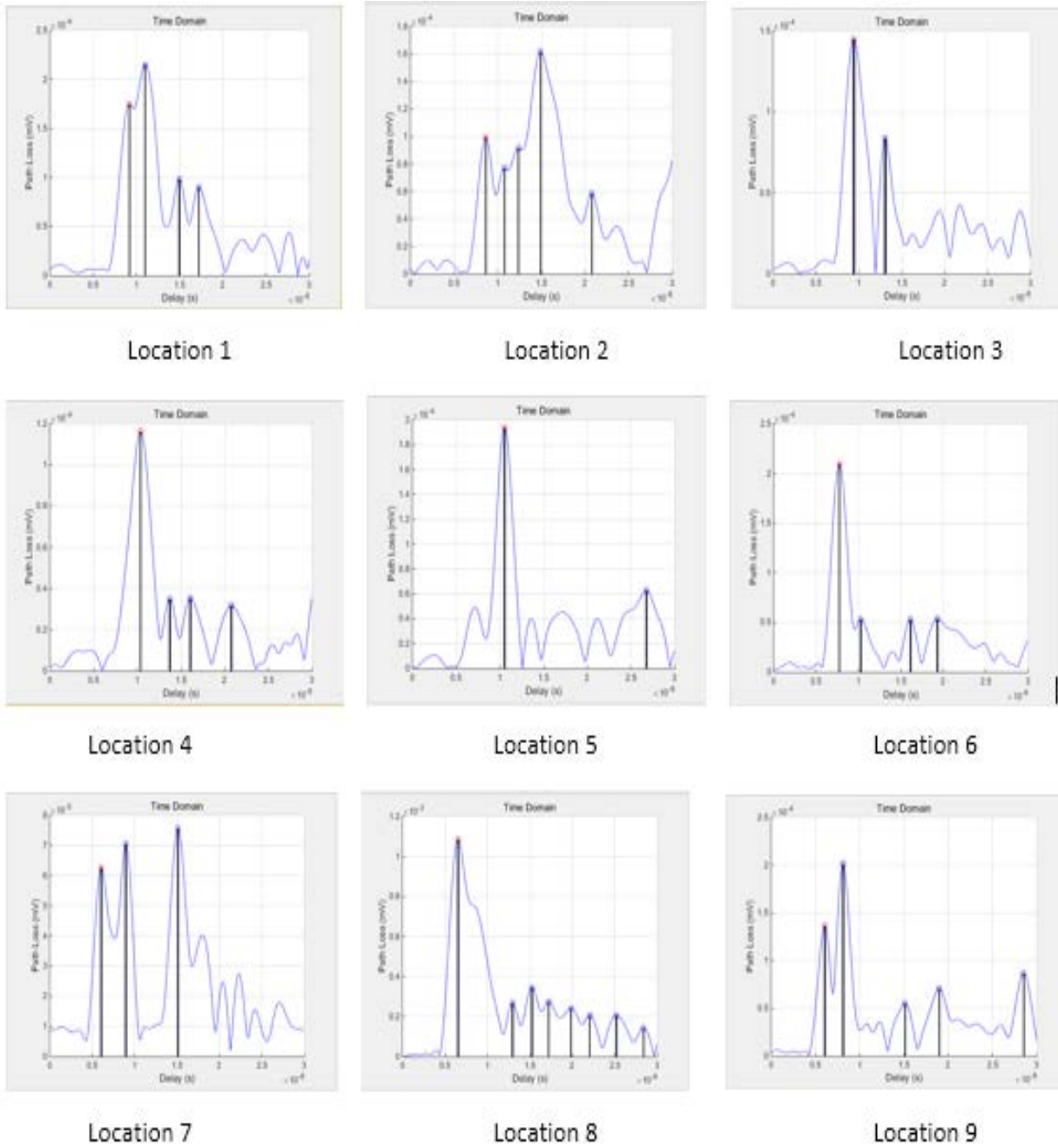


Fig.3.6 Channel profiles of sample measurement in each location with picked peaks for interactive electronic Ping- Pong gaming

3.2 Error Classification

In indoor localization, the localization accuracy suffers from several errors generated by scenario and measurement. Let ϵ represent the total error between the real distance d_r obtained from digital laser measurement, and estimated distance d_e obtained is from $d_e = c\tau_e$, where c is the speed of light and τ_e is the time-of-arrival measured by network analyzer. The total error ϵ is affected by measurement error ϵ_m , multipath effect error ϵ_e and shadow fading error ϵ_s . ϵ_m can be neglected by adding a mounted measurement in free space for every scenario and bandwidth. The result d_0 only includes the measurement error, which means $\epsilon_m = d_0 - d_r$. Therefore, ϵ can be written as

$$\epsilon = |d_0 - d_r + \epsilon_e + \epsilon_s| \quad (1)$$

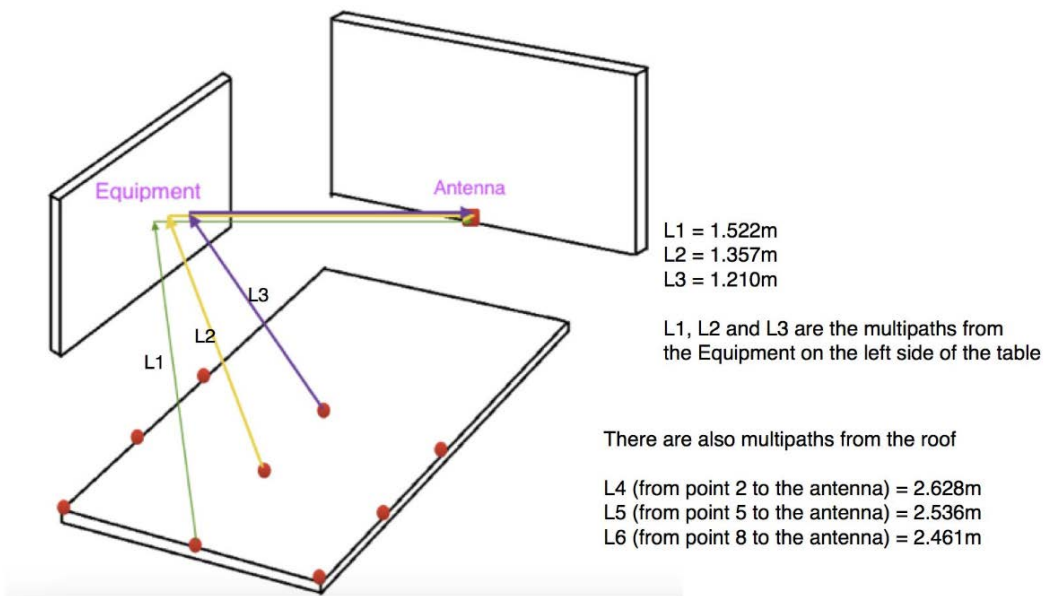
In our scenario, we do static data collection at different positions with different bandwidths, and we get the distance error information is following Gaussian distribution. For this distribution, we will analysis the mean and variance of distance error and try to find out the modeling to define the relationship among mean, variance, multipath, bandwidth and hand cover.

3.3 Modeling on Effect of Multipath

In this section, we do the error modeling on the effect of multipath. In the first part, we give the multipath scenario of the measurement in Figure 3.8. And then we analyze the error of localization on the effect of multipath. The multipath pattern simulation is shown in Figure 3.7.



(a)



(b)

Fig.3.7 Measurement environment multipath model (a) measurement environment in the Lab (b) multipath pattern simulation in measurement scenario

In indoor environment, the alteration of surroundings has big effect on transmitting path, and multipath situation will lead to change of distance error and accuracy. In our scenario, each test point has different multipath situation due to the variety of distance to RX. Therefore, the distance is the main parameter of the change of multipath effect. Since we do measurement statically in each point, we can see the mean of error introduced by different position is little from Figure 3.8 .

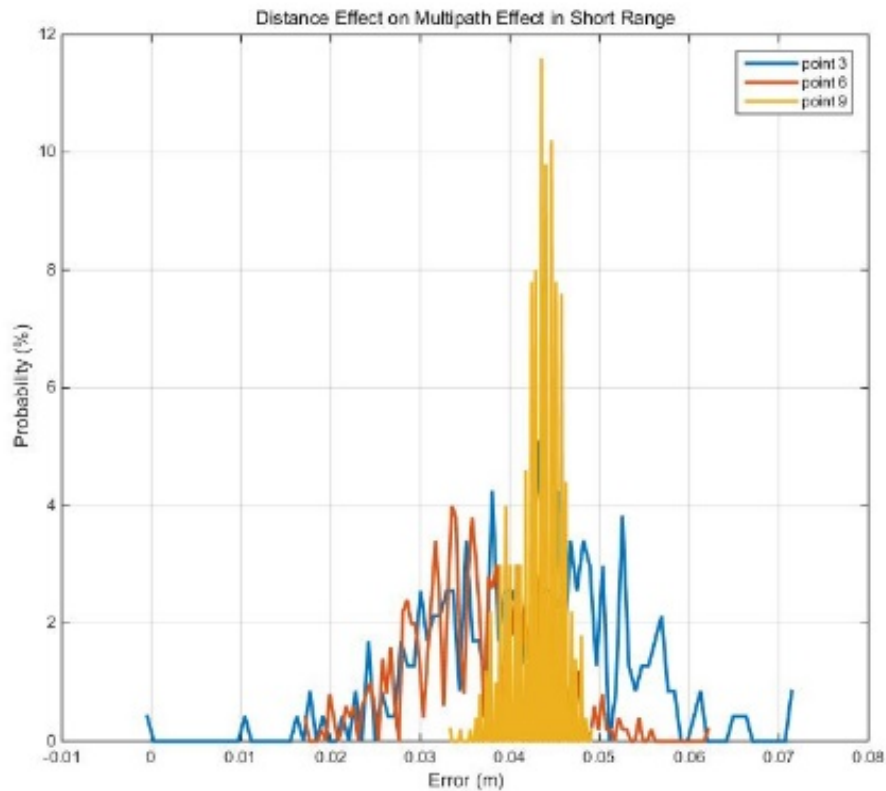


Fig.3.8 PDF of distance measurement error in three different position 3, 6, 9

Figure 3.8 shows us the fact that means of error in different position changes slightly, however, variance changes a lot. Therefore, the multipath effect is mainly concentrating on the variance of error.

Figure 3.9 shows the multipath effect on variance in our indoor short-range localization. The relation can be expressed as

$$\sigma_d^2 = 0.01275d - 0.01607 \quad (2)$$

Where σ_d^2 is the variance of distribution function of distance error distribution, and d is the distance from TX to RX. From this function we can find that the multipath effect in indoor short distance UWB localization is relatively small.

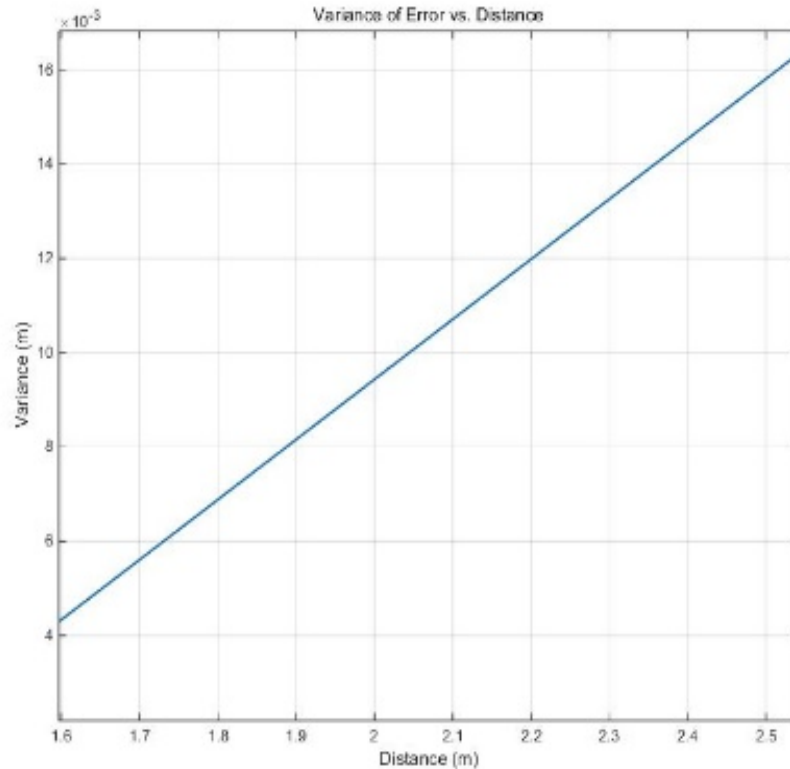


Fig.3.9 Multipath effect on variance, vertical axis is the variance of the distance measurement error and the horizontal axis represents the distance between transmitter and the receiver.

3.4 Modeling on Effect of Human Body

In this section we analysis the localization error on the effect of human body, which means in the condition of LOS and OLOS.

In motion gaming like table tennis, human body always plays an important role in localization error. In Figure 3.10 we can see that the human body has great effect on received power and first peak time in a static point measurement. It contributes to multipath and OLOS by hand covering on the controller's antenna. Figure 3.11 shows the measurement channel profile for a 2GHz bandwidth at 5.5GHz operating frequency. From Figure 3.11 We can see that when we use antenna signal to localize user movement, the effect of hand is obvious and significant. From the channel profile of these two condition, we can see in the LOS condition, it doesn't have few multipath, but in the OLOS, there are many multipath.

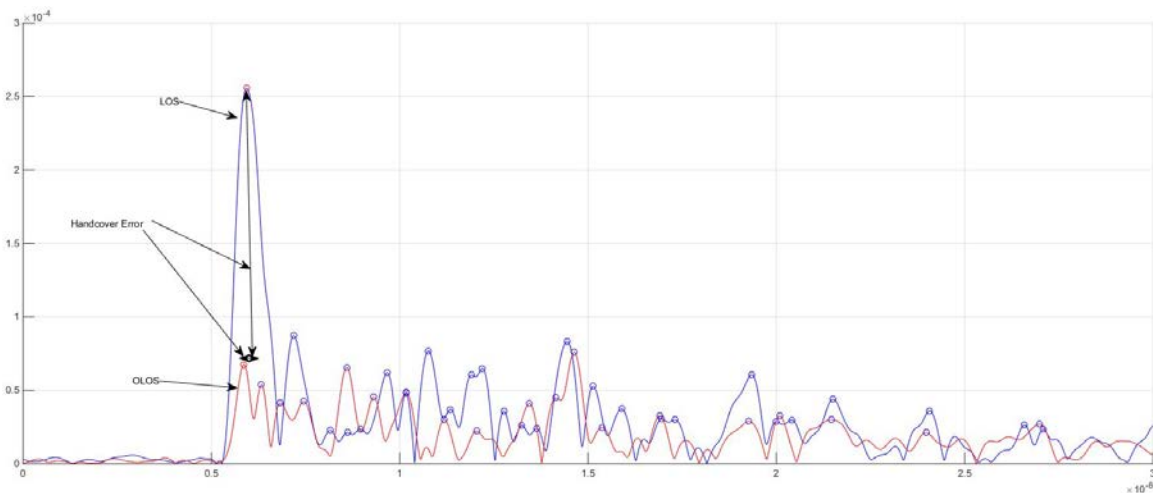
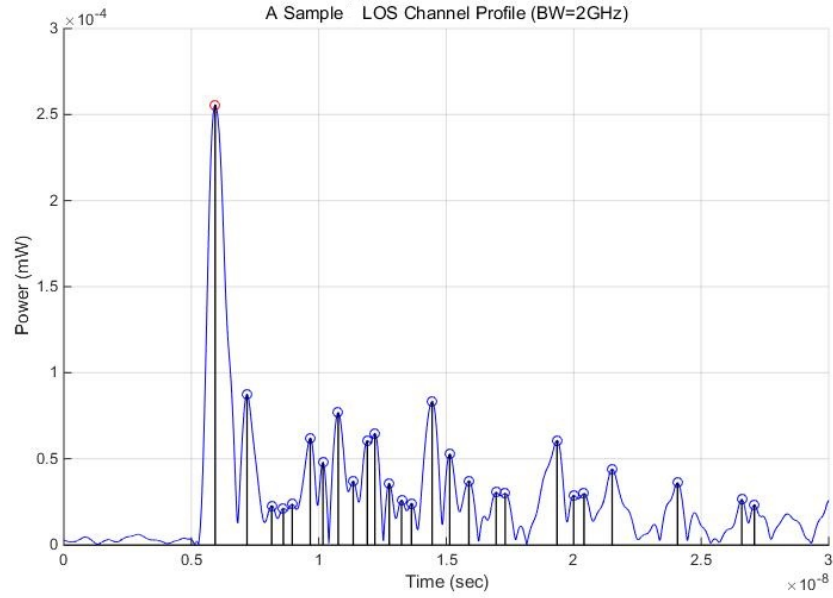
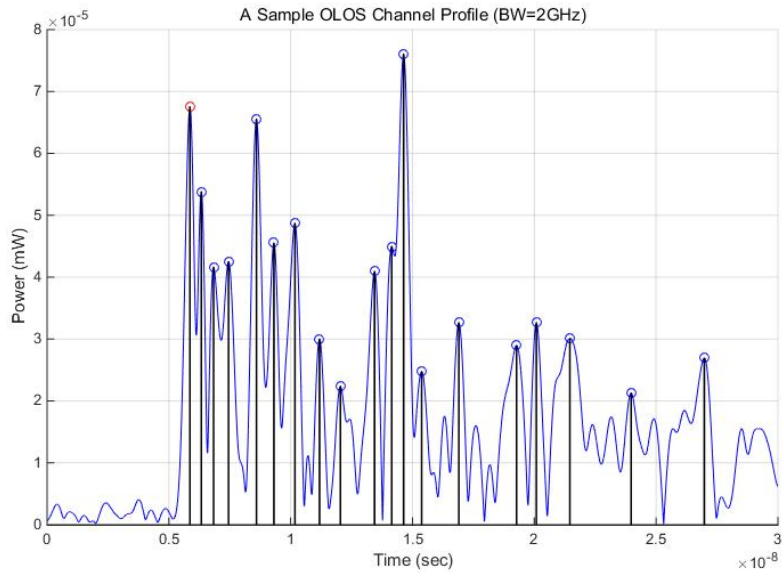


Fig.3.10 Body Effect in Static Point Distance Measurement



(a)



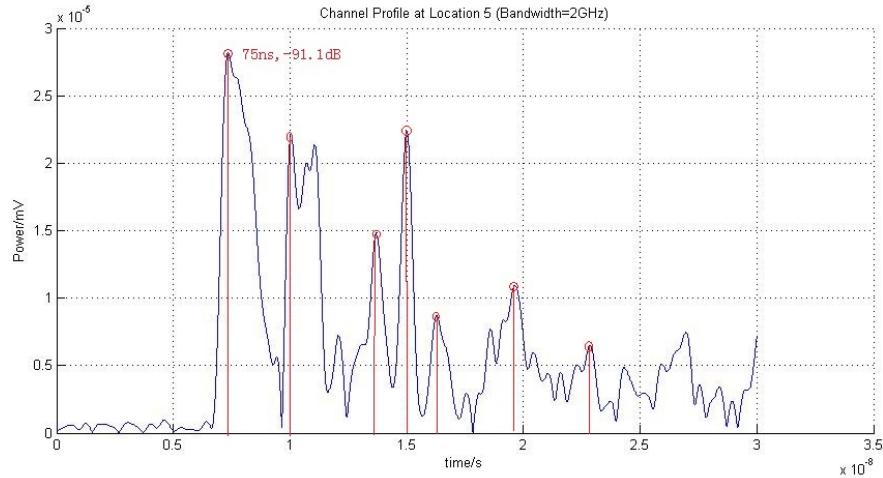
(b)

Fig.3.11 Measurement of channel profile in 2 GHz (a)LOS condition (b)OLOS condition

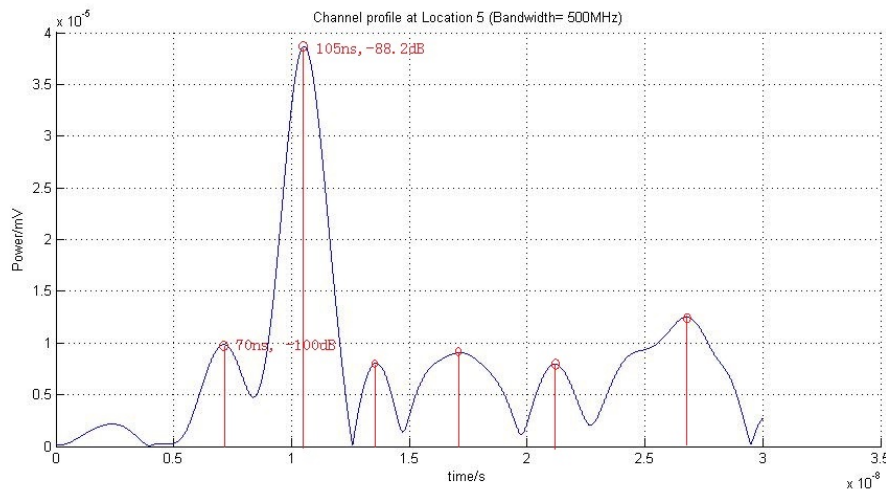
3.5 Modeling on Effect of Bandwidth

After study on multipath and hand cover effect of error, we are going to continue our research on bandwidth effect of distance error. We apply transmitting signal

with bandwidth from 100MHz to 2.5GHz to unfold the secret within bandwidth effect of short-range indoor localization. In Figure 3.12, we show two sample tests with the bandwidth of 2GHz and 500 MHz.



(a)



(b)

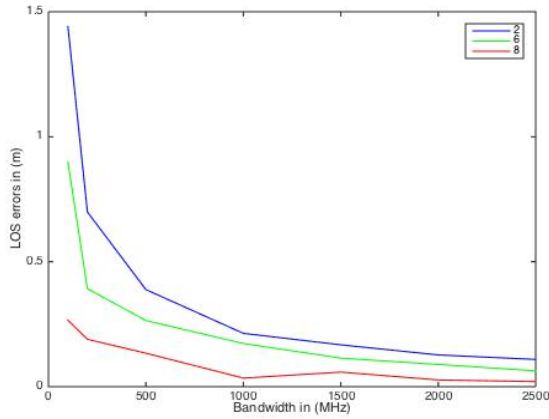
Fig.3.12 Channel profile of two sample tests with operating bandwidth (a)2GHz (b)500MHz

We choose three typical points to do the study on bandwidth. And for these three points, Table I shows the effect of different bandwidth on different location and different hand cover conditions. It contains the mean and variance of error in location 2, 6 and 8 with different operating bandwidths in 100MHz, 200MHz, 500

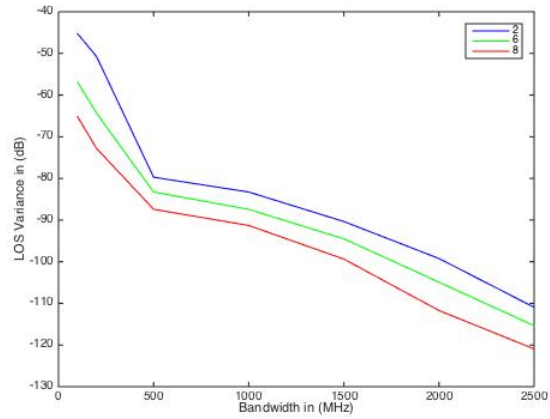
MHz, 1GHz, 1.5GHz, 2GHz and 2.5 GHz. Besides in two conditions, LOS and OLOS. Using the data from Table I, we plot the relationship among these three parameters shown in Figure 3.13.

Table 1 Mean & variance of the ranging error on the effect of operating bandwidth

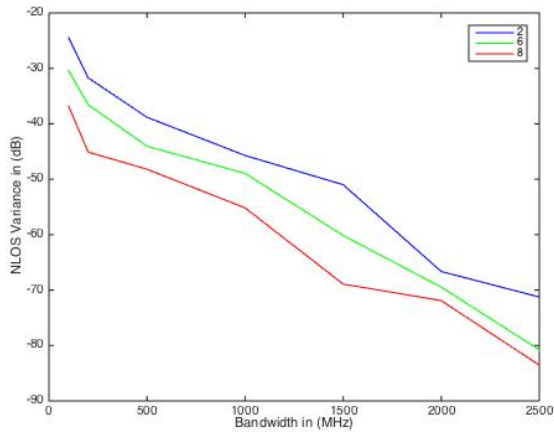
Table 1					
		LOS		OLOS	
		mean error (m)	variance (m)	mean error (m)	variance (m)
100M	2	1.440566237	0.010835961	1.463404187	0.08663919
	6	0.898169857	0.003383556	0.965055099	0.047934583
	8	0.266452792	0.001478321	0.520958815	0.02518481
200M	2	0.698754752	0.006248238	1.089061724	0.041910132
	6	0.391900227	0.001605646	0.692626381	0.025797019
	8	0.189659301	0.000688007	0.252306349	0.010987067
500M	2	0.388388934	3.44860E-04	0.677398825	0.020601318
	6	0.264607214	2.42012E-04	0.38297973	0.012203598
	8	1.33877E-01	1.60E-04	0.162418	0.008067763
1G	2	0.213350613	2.4175E-04	0.368055485	0.010335747
	6	0.173350613	1.59437E-04	0.282952232	7.48314E-03
	8	0.094381234	1.08326E-04	0.130925445	0.004012163
1.5G	2	0.167441797	1.1902E-04	0.324645807	0.006100814
	6	0.114238331	0.000078692	0.204431333	0.002439519
	8	0.058271	0.000048326	0.102936595	0.001015695
2G	2	0.127049728	4.90181E-05	0.292009766	0.001274593
	6	0.08898294	2.77306E-05	0.171567607	9.61108E-04
	8	0.036938211	1.40607E-05	0.095884918	7.54052E-04
2.5G	2	0.108925403	1.51904E-05	0.2459768	0.000804532
	6	0.063387735	9.76020E-06	1.34787E-01	3.09945E-04
	8	0.0203819	5.59250E-06	7.62040E-02	2.35257E-04



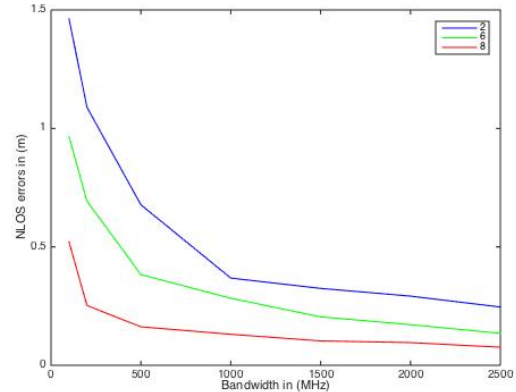
(a)



(b)



(c)



(d)

Fig.3.13 Original relationship between mean & variance of error and operation bandwidth in LOS & OLOS conditions (a) Mean of error in LOS condition (b) Variance of error in LOS condition (c) Mean of error in OLOS condition (d) Variance of error in OLOS condition

After analyzing the original plots in Figure 3.13, we find it is almost an exponential model. So we make a simulation to fit the data and finally come out with an exponential function.

Figure 3.14 and Figure 3.15 are the comparisons of mean and variance of error in LOS and OLOS conditions from 100MHz to 2.5GHz bandwidth. We can see hand cover generate large errors in mean and variance. What's more, with increase of

bandwidth, the accuracy and stability improve a lot. After curve fitting, we generate the function of m_B and σ_B^2 as

$$m_B = \begin{cases} \alpha_L e^{\gamma_L B} + \beta_L e^{\lambda_L B}, LOS \\ \alpha_O e^{\gamma_O B} + \beta_O e^{\lambda_O B}, OLOS \end{cases} \quad (3)$$

$$\sigma_B^2 = \begin{cases} \varphi_L B^{\psi_L} + C_L, LOS \\ \varphi_O B^{\psi_O} + C_O, OLOS \end{cases} \quad (4)$$

Where B is the system-operating bandwidth. The values of these parameter above are got from curve fitting. And the big amount of measurement samples give the idea that for most of the data, we always have $\alpha_O > \alpha_L$, $\varphi_O \gg \varphi_L$ and $\psi_O \approx \psi_L$.

For our case, the value of measurement point 2 is:

$$\alpha_L = 1.277, \beta_L = 1.105e - 03,$$

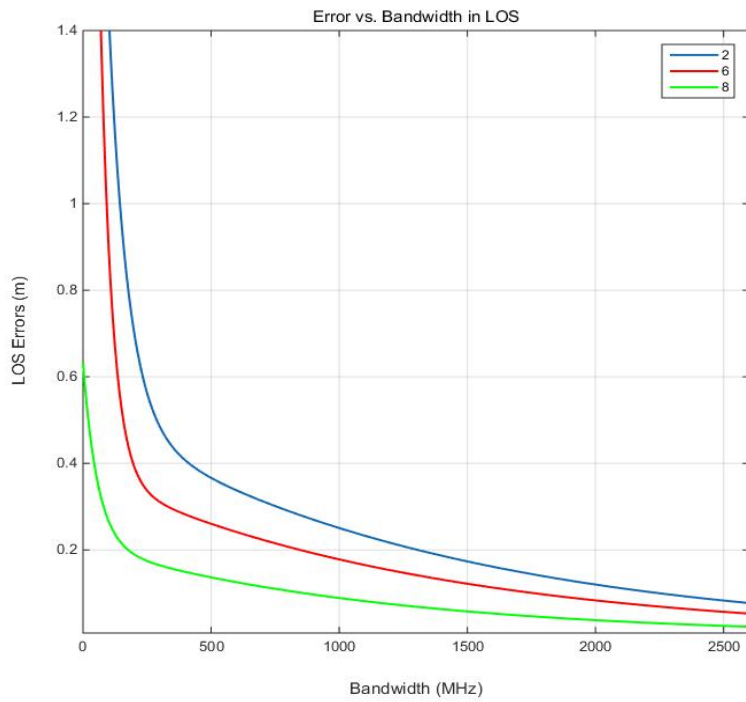
$$\gamma_L = -2.663e - 03, \lambda_L = 9.748e - 04,$$

$$\alpha_O = 1.975, \beta_O = 0.3073,$$

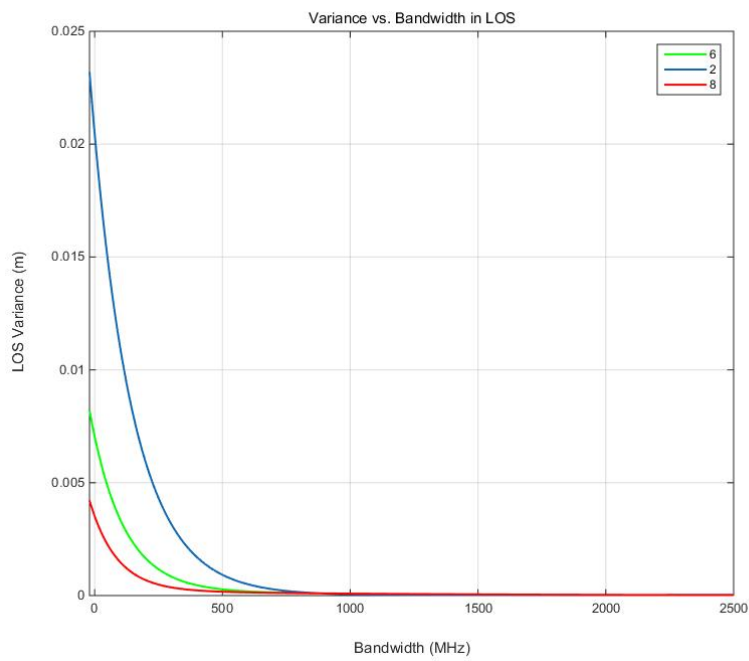
$$\gamma_O = -5.103e - 03, \lambda_O = 2.253e - 05,$$

$$\varphi_L = 19.43, \psi_L = -2.061, C_L = 1.893e - 05,$$

$$\varphi_O = 1.106, \psi_O = -2.304, C_O = 5.759e - 04.$$

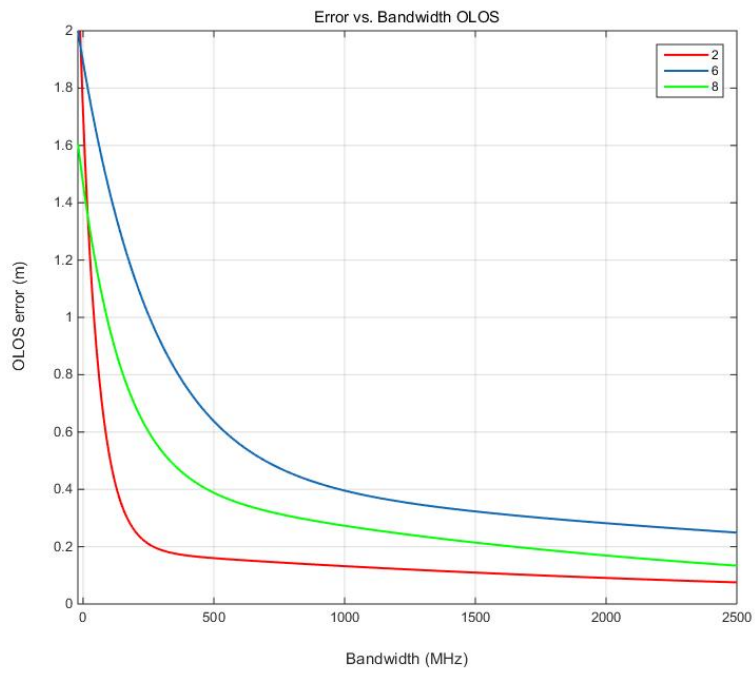


(a)

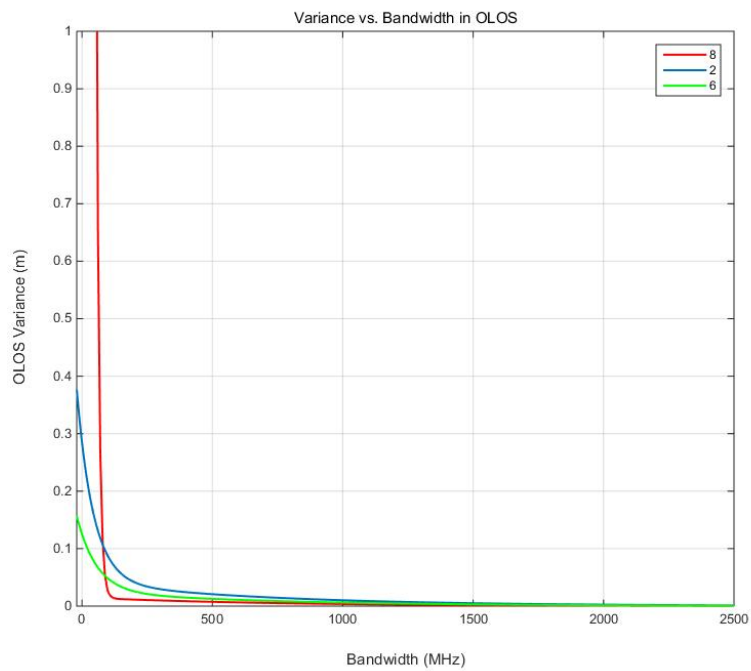


(b)

Fig.3.14 Bandwidth effect on (a)mean and (b)variance of error in LOS conditon in location 2, 6, 8.



(a)



(b)

Fig.3.15 Bandwidth effect on (a)mean and (b)variance of error in OLOS condition in location 2, 6, 8.

By the determination of mean and variance of error, the distance error ϵ now can be expressed as a function of bandwidth and existence of hand cover. The function is given as

$$\epsilon = \frac{1}{(\sigma_B + \sigma_d)\sqrt{2\pi}} e^{-\frac{(x-m_B)^2}{2(\sigma_B^2 + \sigma_d^2)}} \quad (5)$$

And

$$m_B = \begin{cases} \alpha_L e^{\gamma_L B} + \beta_L e^{\lambda_L B}, LOS \\ \alpha_O e^{\gamma_O B} + \beta_O e^{\lambda_O B}, OLOS \end{cases}$$

$$\sigma_B^2 = \begin{cases} \varphi_L B^{\psi_L} + C_L, LOS \\ \varphi_O B^{\psi_O} + C_O, OLOS \end{cases}$$

$$\sigma_d^2 = 0.01275d - 0.01607$$

Where σ_B^2 and σ_d^2 are the variance based on different bandwidths and distances; m_B is the mean of error under different bandwidths.

From this function, we can determine the distance error of indoor localization on UWB when given location, system bandwidth and condition of LOS or OLOS by hand cover. This result can be extended to body area network (BAN) effect on indoor area and upgrading motion gaming system on accuracy by choosing a best-matched parameters. After what we have done right now, we are going to determine other gestures effect on indoor motion gaming localization to find out the effect of other parts of human body. When we finish this task, BAN effect on wireless motion gaming and localization will be determined for any kinds of use depending on detection of human body gestures.

Chapter 4 Micro-Gesture Detection using UWB

Recently, received signal strength (RSS) of the Wi-Fi signals has been used for gesture detection by observing the effects of movements of the arms and legs on the RSS of a Wi-Fi enabled device [69]. In these experiences the radio frequency (RF) antennas are not attached to the human body. Micro-gestures are produced by refined motions of the hand and demand for detection of these refined motions. In this chapter, we introduce a new concept that we refer to as micro-gesture detection to handle the more refined motions of the hand, such as rotation, while one antenna is held by the user and by using four features of the UWB signals. As the hand rotates the position of the antenna in the hand and the external antenna changes from line-of-sight (LOS) to obstructed line-of-sight (OLOS). We demonstrate that features of the UWB signals are more useful than the RSS signal of the Wi-Fi to detect this class of micro-gestures, which can be helpful for the people with limited ability or visually impaired and it may also be applied to some kinds of sign language for the deaf-mute people, which can translate their gestures to help them communicate with others.

In the first section, we present the measurement system and scenario, and then we give the data analysis and results.

4.1 Measurement system and scenario

In this section, we show two measurement systems in Wi-Fi detection and UWB detection. In the first part, we introduce the equipment and software used in the experiment. In the second part, we introduce the two scenarios during the measurement.

4.1.1 Wi-Fi gesture detection

There are some other papers written about using the RSS to do the gesture but WiSee [69] is the most popular one. It is the first wireless system that enables gesture recognition in line-of-sight, non-line-of-sight, and through-the-wall scenarios and they present algorithms to extract gesture information from communication-based wireless signals. Specifically, it shows how to extract minute Doppler shifts from wideband OFDM transmissions that are typical to most modern communication systems including Wi-Fi. The gestures and results of the paper is shown below.

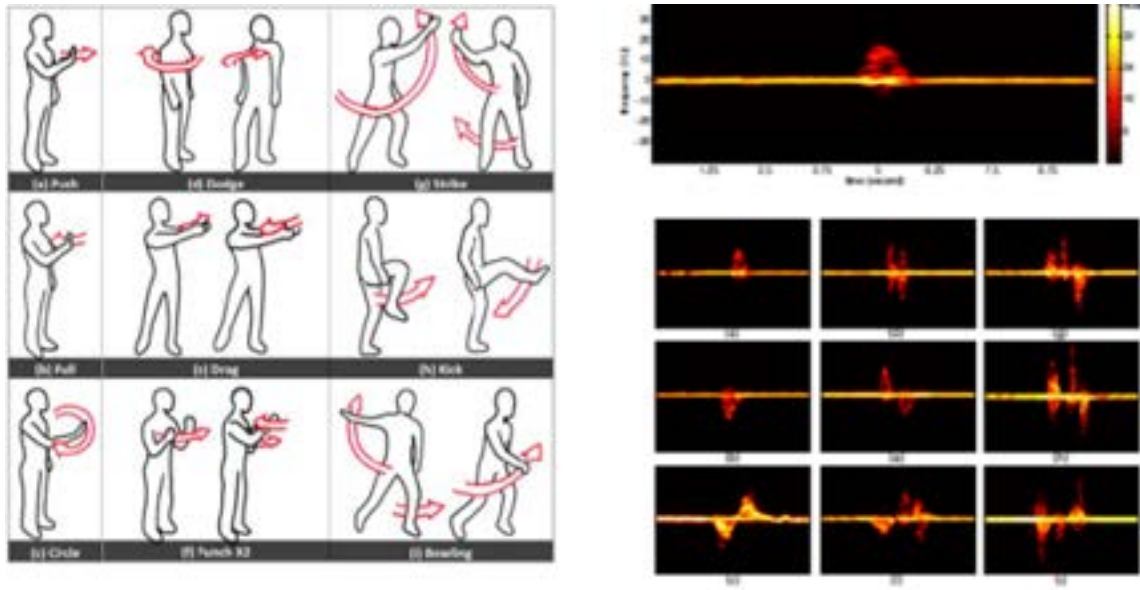


Fig.4.1 Gestures used to detected and results in WiSee [69]

In order to implement the gesture detection mechanism, several challenges have to be addresses. First of all, we need to obtain RSSIs from the Wi-Fi environment, and then extract the movements from RSSI values. Then, we need to map those RSSI characteristics to different gestures.

We use an android phone which has an application (shown in Figure 4.3) used to collect the RSS data from the router (shown in Figure 4.3). The application used in this project is designed by Guanxiong Liu, a former student from CWINS Lab, the code can be seen in his master thesis report [82].We hold the phone in hand, and move up-down, left- right to see how the RSS changes. The distance between the hand and the router is about 1.5m to 2m.

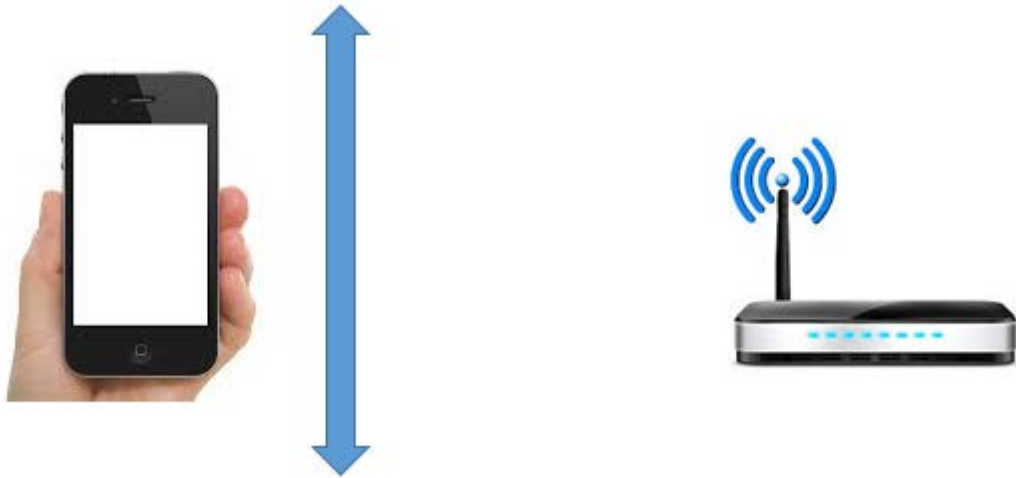


Fig.4.2 Measurement system for Using Wi-Fi signals



Fig.4.3 Application used in the smart phone to collect the RSS data



Fig.4.4 Router used to generate Wi-Fi signal

4.1.2 UWB gesture detection

Two possible scenarios as well as gestures have been introduced in our measurement. The first one is LOS condition (Line-of-sight propagation is a characteristic of electromagnetic radiation or acoustic wave propagation. Electromagnetic transmission includes light emissions traveling in a straight line. The rays or waves may be diffracted, refracted, reflected, or absorbed by atmosphere and obstructions with material and generally cannot travel over the horizon or behind obstacles.), which the receiving antenna attached to the hand has a direct line of site to the transmitter on the shelf.

The second case is the OLOS condition (Obstacle-line of sight or Non-line-of-sight is radio transmission across a path that is partially obstructed, usually by a physical object in the innermost Fresnel zone) where the user turns over the hand or obstructs the LOS by putting hand behind the body.

To measure the behavior of target node and base stations, a vector network analyzer has been employed in our measurement system. The measurements were carried out in the Atwater Kent Laboratory of Worcester Polytechnic Institute, using two UWB directional antennas, which have been connected to both transmit and receive port of the network analyzer through low loss RF cables. Moreover, a power amplifier has been added at the transmitter (TX) port of network analyzer to achieve better signal to noise ratio (SNR) at the receiver (RX) side. We use two UWB directional antennas (shown in Figure 4.6) that have been connected to both transmit and receive port of the network analyzer through low loss RF cables as shown in Figure 4.5. The vary frequency of operation of the network analyzer is from 3 GHz to 8GHz. In Figure 4.7, we show two sample measurement results in two different gestures.

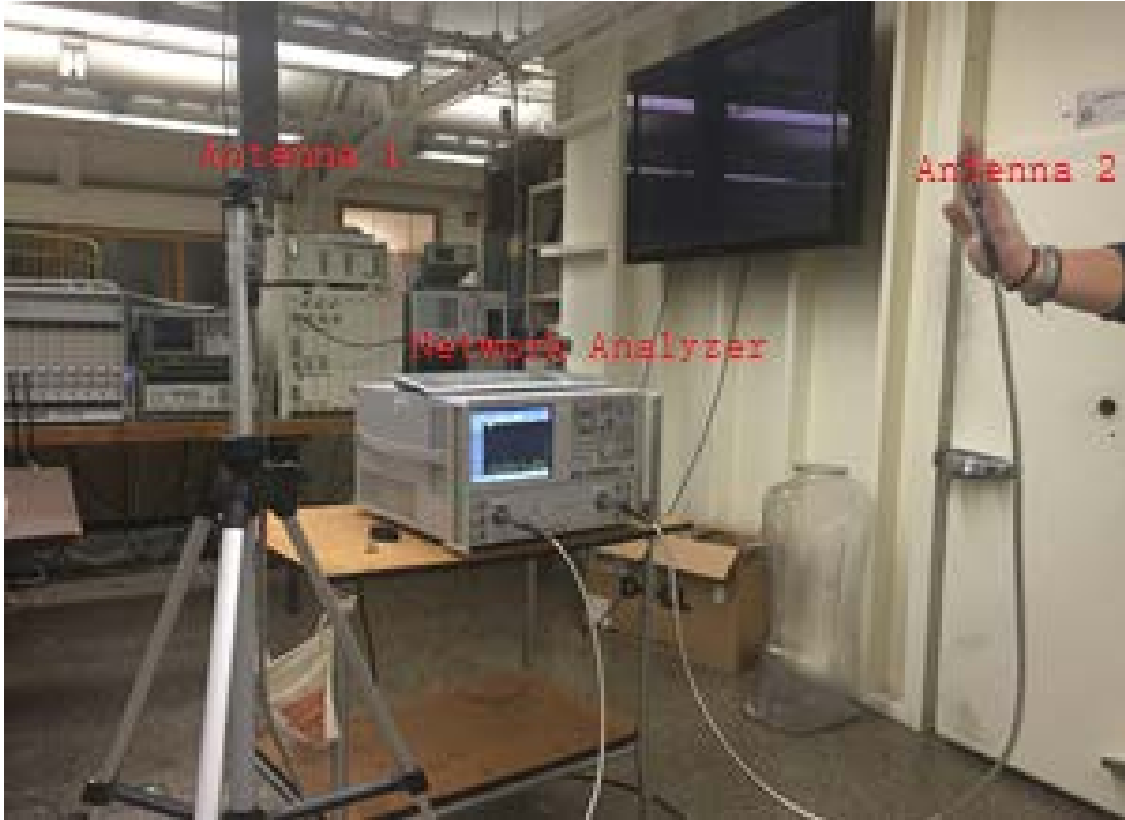
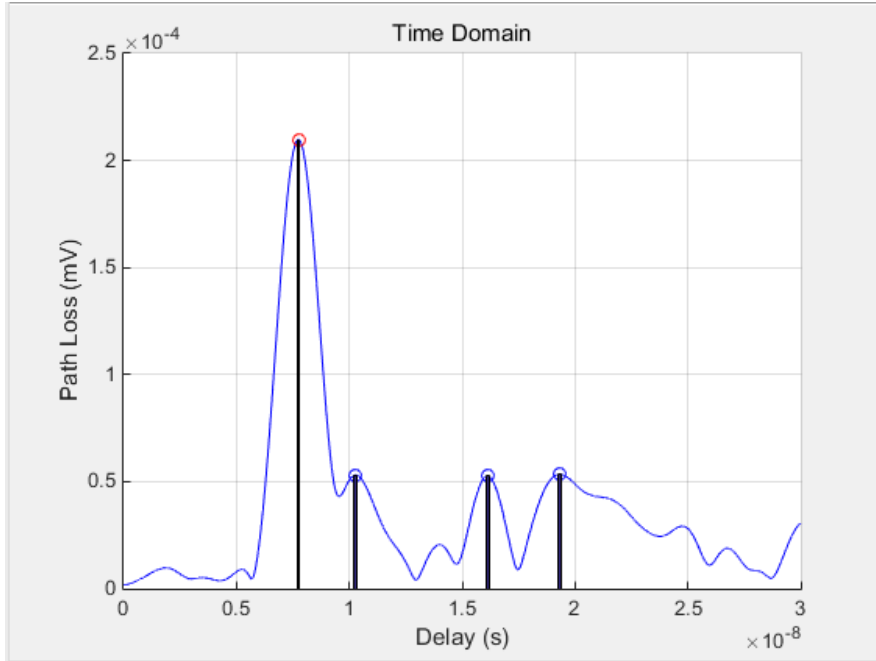


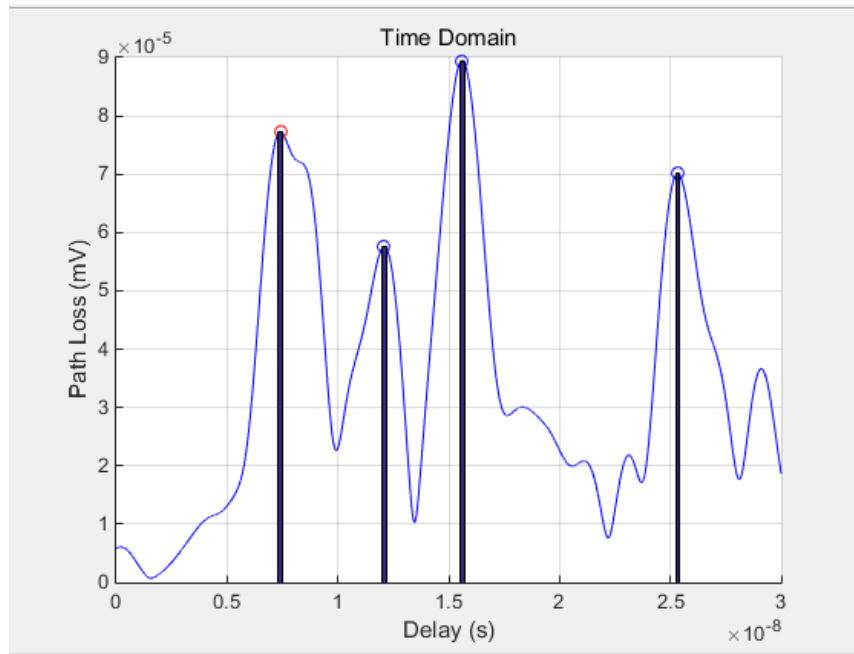
Fig.4.5 Measurement system for using UWB signals



Fig.4.6 The UWB directional antenna



(a)



(b)

Fig.4.7 Sample of the measurement in two gestures (a) Gesture 1(b) Gesture 2

4.2 Data analysis and results

In this section, we present the results of gesture detection using both Wi-Fi and UWB. After that, we make a compare between them.

In the gesture detection using Wi-Fi signal, we can have the statistics of RSS and use their spectrograms to detect different gesture, up down and right left. From Figure 4.8 (a) and 4.8 (b), we can see that the RSS separately in up and down, it increases from -31dB to -27dB in Up and opposites in Down. In Figure 4.8 (c), the RSS first raise then decline when in the gesture up-down, but the gap is just 4dB; and 4.8 (d), the RSS first increase sand then decreases in the gesture right-left, the gap is only 2dB.

Due to Figure 4.8, we can see the difference between each gesture is not very clear. However, so there is a major challenge for accurate positioning due to the dynamic and unpredictable nature of radio channel, such as shadowing, multipath, orientation of the wireless device. [83]

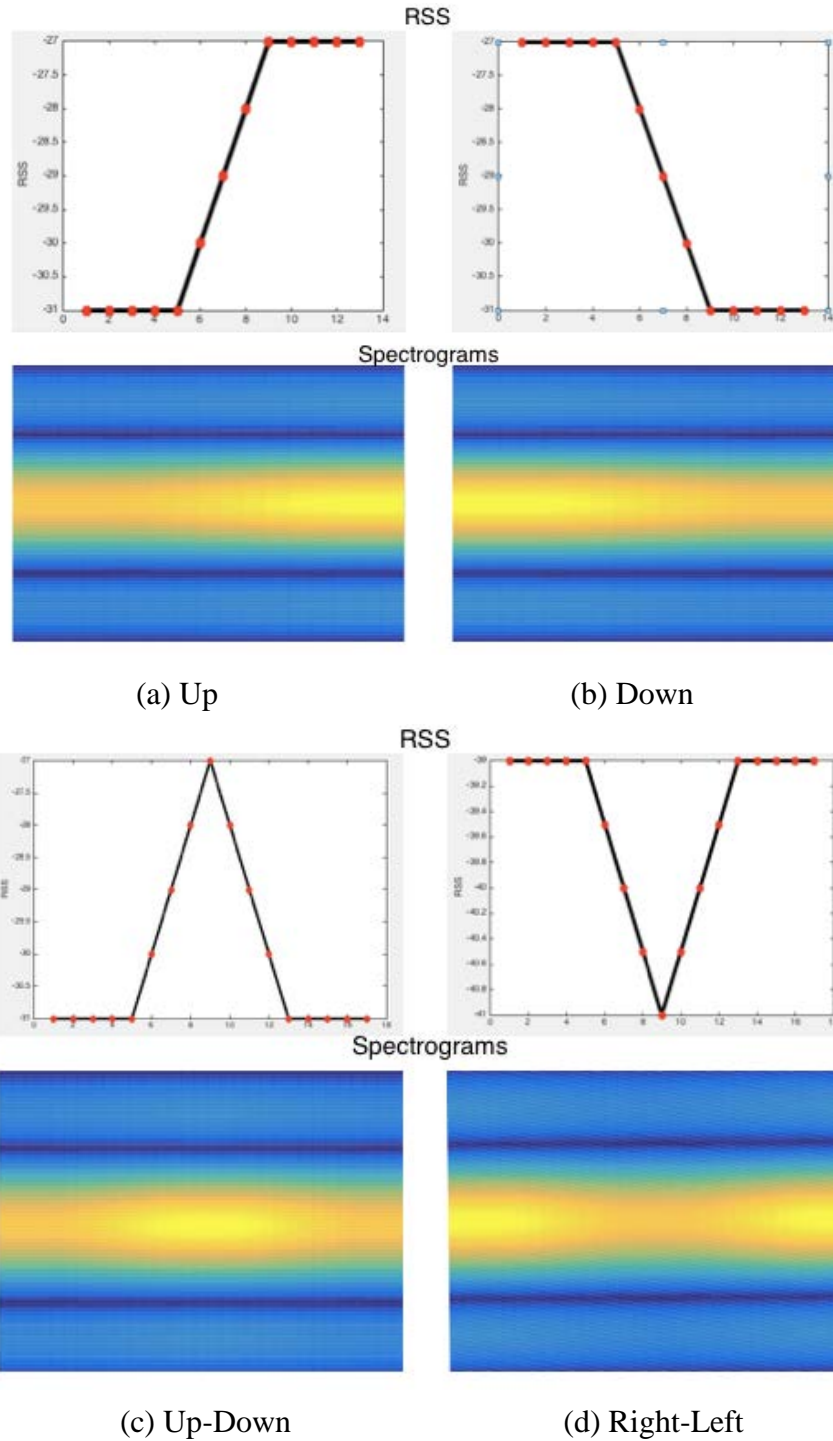
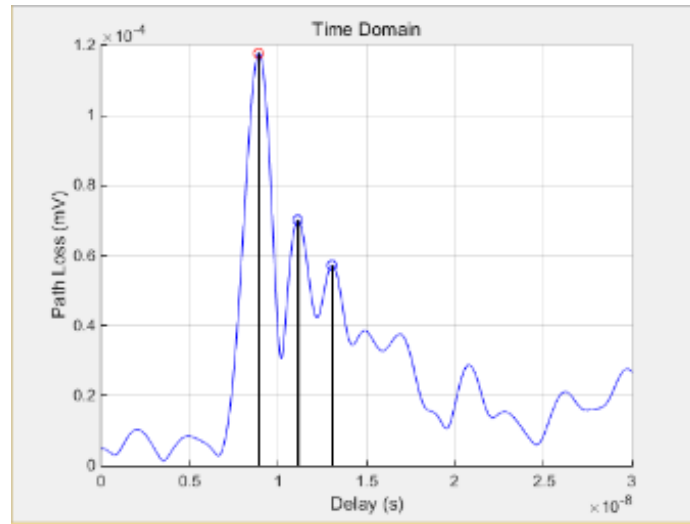


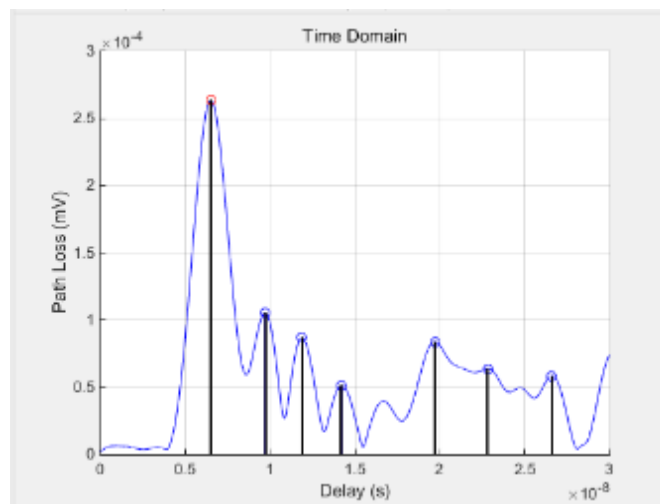
Fig.4.8 Different hand gestures' RSS and spectrograms.

For the gesture detection using UWB signals, we have totally four parameters: time of arrival, first peak power, total power and the RMS delay spread [84]. We

will discuss them one by one. When blind people wave his hand, the distance between the two sensors will change, which will directly affect the TOA. Figure 4.9 shows two profiles when the distance changes. In Position 1, the time of arrival is about 8.5ns; in Position 2, the time of arrival is about 6.5ns. Since the TOA changes can easily be detected, the changes in distance are obviously shown.



(a)



(b)

Fig.4.9 Profile distributions of two different positions(a) Position 1(b) Position 2

Besides, if visually impaired want to change the channel of radio or music player, he can just turnover or put his hand behind his body, to be an OLOS condition, then this geature can be detected. We use τ_{rms} (the root mean square delay spread) to as TOA detection of hand gesture change. τ_{rms} is a value generated from multipath environment [85], which can be express as

$$\tau_{rms} = \sqrt{\overline{\tau^2} - (\overline{\tau})^2} \quad (6)$$

$$\overline{\tau^n} = \frac{\sum_{i=1}^L \tau_i^n |\beta_i|^2}{\sum_{i=1}^L |\beta_i|^2} \quad n=1, 2 \quad (7)$$

In these functions, τ_i is the time delay in different transmitting paths, and $|\beta_i|^2$ is the corresponding peak power of each τ_i , n is the number of all paths in the measurement environment.

From Figure 4.10, we can find the mean of τ_{rms} separated in two clusters of LOS and OLOS. The expression of TOA method can be expressed as

$$\tau_{rms}(\text{LOS}) = \tau_{rms}(\text{OLOS}) + \tau_{\text{gap}} \quad (8)$$

Where $\tau_{rms}(\text{LOS})$ is the root mean square of delay spread of LOS, $\tau_{rms}(\text{OLOS})$ is the root mean square of delay spread of OLOS, and τ_{gap} is the time gap from LOS to OLOS, $\tau_{\text{gap}} \in (0.5\text{ns}, 1\text{ns})$.

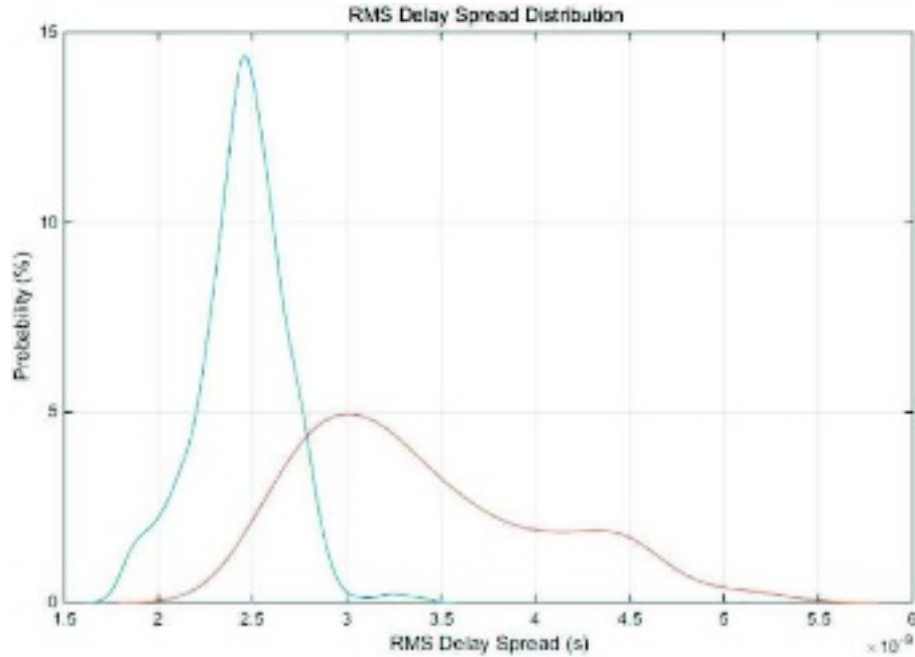


Fig.4.10 Mean of τ_{rms} and received in LOS and OLOS

Using UWB signals, we can also do the detection by according to the first peak power. Figure 4.11 shows the channel profile of both LOS and OLOS conditions, there is a huge decrease of the first peak power from LOS to OLOS. The power in LOS is about three times larger than it is in OLOS.

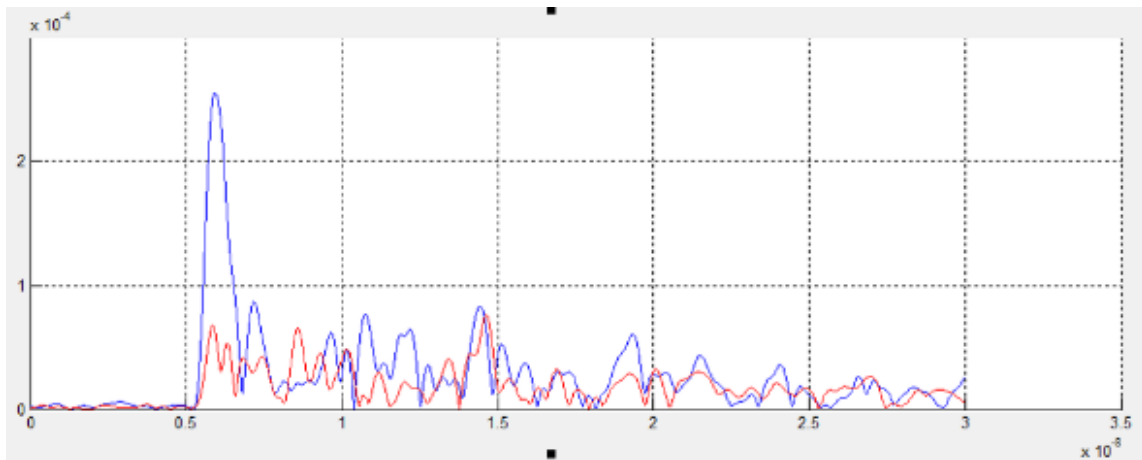


Fig.4.11 First peak power in LOS and OLOS scenarios

Moreover, the difference of power does not only occurs in the first peak, but also in the total power. The total power is the sum of power of peaks over given threshold. The value of total power shows the signal strength received by receiver. From the waveform of two scenarios in Figure 4.12, we can see that the total power of OLOS is dramatically smaller than LOS condition. From the measurement data, we find out that there is a statistical mean of power drop from LOS to OLOS. The relation can be expressed as

$$m_{\text{power}}(\text{LOS}) = m_{\text{power}}(\text{OLOS}) + P_{\text{gap}} \quad (9)$$

Where $m_{\text{power}}(\text{LOS})$ is the mean of total power of LOS, $m_{\text{power}}(\text{OLOS})$ is the mean of total power of OLOS, and P_{gap} is the power gap from LOS to OLOS. Note that $P_{\text{gap}} \in (6\text{mW}, 12\text{mW})$.

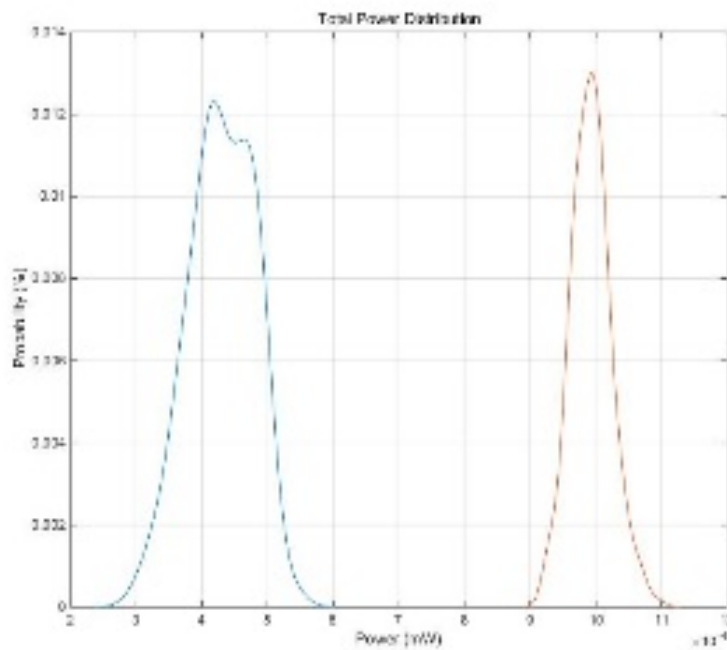


Fig.4.12 Total power in LOS and OLOS scenarios

By determining all the parameters shown in front, we can detect gestures and movements. Identifying little movement like hand turnover or put hand behind the body, which is very common in our daily life, but it will improve the quality of visually impaired life and even the medical applications using gesture detection.

Chapter 5 Conclusions and future work

In this thesis, we first introduced channel models for statistical behavior of localization error due to multipath, different operating bandwidths and the obstruction of motion controller antenna for indoor electronic Ping-Pang gaming. We built a database by performing 500 measurements on 9 locations using different operating bandwidths in LOS and OLOS two scenarios. Using empirical results of UWB channel measurements in indoor localization, we found our model closely fit the result of measurements. The models can help to improve the localization accuracy, agility, broaden the field of application for typical indoor motion gaming system.

Then, we compared the gesture detection using RSS of Wi-Fi signal and gesture detection using four characteristics of UWB signals, which is more accurate and reliable. The result of UWB micro-gesture detection will be helpful for the people with limited mobility or visually impaired for implementation of simplified sign languages to communication with electronic devices located away from the person.

We are going to continue our research in three aspects. Firstly, the multipath profiles, which we make a compare between the one in the typical indoor environment and in the chamber to see how long the multipath is and if it fits the real environment or not. Secondly, by using UWB technology, we want to detect

more gestures and find out if we can use it to detect the speed and the direction of the motion. Thirdly, we want to use our conclusions to find more applications of UWB localization and gesture detection.

Reference

- [1] Lange, B., Chang, C. Y., Suma, E., Newman, B., Rizzo, A. S., & Bolas, M. (2011, August). Development and evaluation of low cost game-based balance rehabilitation tool using the Microsoft Kinect sensor. In *Engineering in Medicine and Biology Society, EMBC, 2011 Annual International Conference of the IEEE* (pp. 1831-1834). IEEE.
- [2] Bharath, L., Shashank, S., Nageli, V. S., Shrivastava, S., & Rakshit, S. (2010, December). Tracking method for human computer interaction using Wii remote. In *Emerging Trends in Robotics and Communication Technologies (INTERACT), 2010 International Conference on* (pp. 133-137). IEEE.
- [3] Geng, Y., He, J., Deng, H., & Pahlavan, K. (2013, June). Modeling the effect of human body on TOA ranging for indoor human tracking with wrist mounted sensor. In *Wireless Personal Multimedia Communications (WPMC), 2013 16th International Symposium on* (pp. 1-6). IEEE.
- [4] Schou, T., & Gardner, H. J. (2007, November). A Wii remote, a game engine, five sensor bars and a virtual reality theatre. In *Proceedings of the 19th Australasian conference on Computer-Human Interaction: Entertaining User Interfaces* (pp. 231-234). ACM.
- [5] Odijk, D., & Tiberius, C. C. J. M. (2006). Assessing the accuracy of high sensitivity GPS receiver for location based services. *Proceeding of NaviTec, Estec, Noordwijk, The Netherlands*, 11-14.
- [6] Li, X., & Pahlavan, K. (2004). Super-resolution TOA estimation with diversity for indoor geolocation. *Wireless Communications, IEEE Transactions on*, 3(1), 224-234.
- [7] Gezici, S., Tian, Z., Giannakis, G. B., Kobayashi, H., Molisch, A. F., Poor, H. V., & Sahinoglu, Z. (2005). Localization via ultra-wideband radios: a look at positioning aspects for future sensor networks. *Signal Processing Magazine, IEEE*, 22(4), 70-84.
- [8] Pahlavan, K., Krishnamurthy, P., & Beneat, J. (1998). Wideband radio propagation modeling for indoor geolocation applications. *Communications Magazine, IEEE*, 36(4), 60-65.
- [9] Pahlavan, K., & Levesque, A. H. (2005). *Wireless information networks* (Vol. 93). John Wiley & Sons.
- [10] Zand, E. D., Pahlavan, K., & Beneat, J. (2003, September). Measurement of TOA using frequency domain characteristics for indoor geolocation. In *Personal, Indoor and Mobile Radio Communications, 2003. PIMRC 2003. 14th IEEE Proceedings on* (Vol. 3, pp. 2213-2217). IEEE.

- [11] Leder, R. S., Azcarate, G., Savage, R., Savage, S., Sucar, L. E., Reinkensmeyer, D., ... & Molina, A. (2008, August). Nintendo Wii remote for computer simulated arm and wrist therapy in stroke survivors with upper extremity hemiparesis. In *Virtual Rehabilitation, 2008* (pp. 74-74). IEEE.
- [12] Kreylos, O. (2008). Oliver kreylos' research and development homepage-wiimote hacking. Accessed Sep, 15.
- [13] Choe, S. B., & Faraway, J. J. (2004). Modeling head and hand orientation during motion using quaternions. *SAE transactions*, 113(1), 186-192.
- [14] Lee, J. C. (2008). Hacking the nintendo wii remote. *Pervasive Computing, IEEE*, 7(3), 39-45.
- [15] <http://news.softpedia.com/news/Accelerometers-in-One-of-Three-Phones-by-2010-116360.shtml>
- [16] https://upload.wikimedia.org/wikipedia/commons/3/35/Gyroscope_wheel-text.png
- [17] https://en.wikipedia.org/wiki/Image_sensor
- [18] Zhang, Z. (2012). Microsoft kinect sensor and its effect. *MultiMedia, IEEE*, 19(2), 4-10.
- [19] Nishikawa, A., Hosoi, T., Koara, K., Negoro, D., Hikita, A., Asano, S., ... & Miyake, Y. (2003). FAcE MOUSe: A novel human-machine interface for controlling the position of a laparoscope. *Robotics and Automation, IEEE Transactions on*, 19(5), 825-841.
- [20] Wachs, J. P., Kölsch, M., Stern, H., & Edan, Y. (2011). Vision-based hand-gesture applications. *Communications of the ACM*, 54(2), 60-71.
- [21] Feng, C., Valaee, S., Au, A. W. S., Reyes, S., Sorour, S., Markowitz, S. N., ... & Eizenman, M. (2012). Anonymous Indoor Navigation System on Handheld Mobile Devices for Visually Impaired. *International Journal of Wireless Information Networks*, 19(4), 352-367.
- [22] Wachs, J. P., Stern, H. I., Edan, Y., Gillam, M., Handler, J., Feied, C., & Smith, M. (2008). A hand gesture sterile tool for browsing MRI images in the OR. *Journal of the American Medical Informatics Association*, M2410v1.
- [23] Graetzel, C., Fong, T., Grange, S., & Baur, C. (2004). A non-contact mouse for surgeon-computer interaction. *Technology and Health Care*, 12(3), 245-257.
- [24] Lukowicz, F., Timm-Giel, A., Lawo, M., & Herzog, O. (2007). Wearit@ work: Toward real-world industrial wearable computing. *Pervasive Computing, IEEE*, 6(4), 8-13.

- [25] Kuno, Y., Murashina, T., Shimada, N., & Shirai, Y. (2000). Intelligent wheelchair remotely controlled by interactive gestures. In *Pattern Recognition, 2000. Proceedings. 15th International Conference on* (Vol. 4, pp. 672-675). IEEE.
- [26] Ferrell, W. R., & Sheridan, T. B. (1963). Remote manipulative control with transmission delay.
- [27] Becker, D. A., & Pentland, A. (1996, August). Staying alive: A virtual reality visualization tool for cancer patients. In *AAAI Workshop on Entertainment and Alife/AI* (pp. 17-21).
- [28] Gutiérrez, M., Lemoine, P., Thalmann, D., & Vexo, F. (2004, November). Telerehabilitation: controlling haptic virtual environments through handheld interfaces. In *Proceedings of the ACM symposium on Virtual reality software and technology* (pp. 195-200). ACM.
- [29] Gutiérrez, M., Lemoine, P., Thalmann, D., & Vexo, F. (2004, November). Telerehabilitation: controlling haptic virtual environments through handheld interfaces. In *Proceedings of the ACM symposium on Virtual reality software and technology* (pp. 195-200). ACM.
- [30] Patel, R., & Roy, D. (1998). Teachable interfaces for individuals with dysarthric speech and severe physical disabilities. In *Proceedings of the AAAI Workshop on Integrating Artificial Intelligence and Assistive Technology* (pp. 40-47). Madison, WI: AAAI Press.
- [31] Boian, R., Sharma, A., Han, C., Merians, A., Burdea, G., Adamovich, S., ... & Poizner, H. (2002). Virtual reality-based post-stroke hand rehabilitation. *Studies in health technology and informatics*, 64-70.
- [32] Soutschek, S., Penne, J., Hornegger, J., & Kornhuber, J. (2008, June). 3-d gesture-based scene navigation in medical imaging applications using time-of-flight cameras. In *Computer Vision and Pattern Recognition Workshops, 2008. CVPRW'08. IEEE Computer Society Conference on* (pp. 1-6). IEEE.
- [33] Krapichler, C., Haubner, M., Engelbrecht, R., & Englmeier, K. H. (1998). VR interaction techniques for medical imaging applications. *Computer methods and programs in biomedicine*, 56(1), 65-74.
- [34] Schlömer, T., Poppinga, B., Henze, N., & Boll, S. (2008, February). Gesture recognition with a Wii controller. In *Proceedings of the 2nd international conference on Tangible and embedded interaction* (pp. 11-14). ACM.
- [35] Lara, O. D., & Labrador, M. A. (2013). A survey on human activity recognition using wearable sensors. *Communications Surveys & Tutorials, IEEE*, 15(3), 1192-1209.

- [36] Hao, T., Xing, G., & Zhou, G. (2013, November). iSleep: unobtrusive sleep quality monitoring using smartphones. In *Proceedings of the 11th ACM Conference on Embedded Networked Sensor Systems* (p. 4). ACM.
- [37] Qi, X., Keally, M., Zhou, G., Li, Y., & Ren, Z. (2013, April). AdaSense: Adapting sampling rates for activity recognition in Body Sensor Networks. In *Real-Time and Embedded Technology and Applications Symposium (RTAS), 2013 IEEE 19th* (pp. 163-172). IEEE.
- [38] Keally, M., Zhou, G., Xing, G., Wu, J., & Pyles, A. (2011, November). Pbn: towards practical activity recognition using smartphone-based body sensor networks. In *Proceedings of the 9th ACM Conference on Embedded Networked Sensor Systems* (pp. 246-259). ACM.
- [39] Cheng, H. T., Sun, F. T., Griss, M., Davis, P., Li, J., & You, D. (2013, June). Nuactiv: Recognizing unseen new activities using semantic attribute-based learning. In *Proceeding of the 11th annual international conference on Mobile systems, applications, and services* (pp. 361-374). ACM.
- [40] Aminian, K., Dadashi, F., Mariani, B., Lenoble-Hoskovec, C., Santos-Eggimann, B., & Büla, C. J. (2014, September). Gait analysis using shoe-worn inertial sensors: how is foot clearance related to walking speed?. In *Proceedings of the 2014 ACM International Joint Conference on Pervasive and Ubiquitous Computing* (pp. 481-485). ACM.
- [41] Maekawa, T., Kishino, Y., Sakurai, Y., & Suyama, T. (2013). Activity recognition with hand-worn magnetic sensors. *Personal and ubiquitous computing*, 17(6), 1085-1094.
- [42] Yürüten, O., Zhang, J., & Pu, P. H. (2014, April). Predictors of life satisfaction based on daily activities from mobile sensor data. In *Proceedings of the SIGCHI Conference on Human Factors in Computing Systems* (pp. 497-500). ACM.
- [43] Schuldhaus, D., Leutheuser, H., & Eskofier, B. M. (2013, September). Classification of daily life activities by decision level fusion of inertial sensor data. In *Proceedings of the 8th International Conference on Body Area Networks* (pp. 77-82). ICST (Institute for Computer Sciences, Social-Informatics and Telecommunications Engineering).
- [44] Mokaya, F. O., Nguyen, B., Kuo, C., Jacobson, Q., Rowe, A., & Zhang, P. (2013, April). Mars: a muscle activity recognition system enabling self-configuring musculoskeletal sensor networks.

- In *Proceedings of the 12th international conference on Information processing in sensor networks* (pp. 191-202). ACM.
- [45] Ke, S. R., Thuc, H. L. U., Lee, Y. J., Hwang, J. N., Yoo, J. H., & Choi, K. H. (2013). A review on video-based human activity recognition. *Computers*,2(2), 88-131.
- [46] Ren, X., & Gu, C. (2010). Figure-ground segmentation improves handled object recognition in egocentric video..
- [47] Messing, R., Pal, C., & Kautz, H. (2009, September). Activity recognition using the velocity histories of tracked keypoints. In *Computer Vision, 2009 IEEE 12th International Conference on* (pp. 104-111). IEEE.
- [48] Shotton, J., Sharp, T., Kipman, A., Fitzgibbon, A., Finocchio, M., Blake, A., ... & Moore, R. (2013). Real-time human pose recognition in parts from single depth images. *Communications of the ACM*, 56(1), 116-124.
- [49] Oikonomidis, I., Kyriazis, N., & Argyros, A. A. (2011, August). Efficient model-based 3D tracking of hand articulations using Kinect. In *Bmvc* (Vol. 1, No. 2, p. 3).
- [50] Lei, J., Ren, X., & Fox, D. (2012, September). Fine-grained kitchen activity recognition using rgb-d. In *Proceedings of the 2012 ACM Conference on Ubiquitous Computing* (pp. 208-211). ACM.
- [51] Buettner, M., Prasad, R., Philipose, M., & Wetherall, D. (2009, September). Recognizing daily activities with RFID-based sensors. In *Proceedings of the 11th international conference on Ubiquitous computing* (pp. 51-60). ACM.
- [52] Hevesi, P., Wille, S., Pirkl, G., Wehn, N., & Lukowicz, P. (2014, September). Monitoring household activities and user location with a cheap, unobtrusive thermal sensor array. In *Proceedings of the 2014 ACM international joint conference on pervasive and ubiquitous computing* (pp. 141-145). ACM.
- [53] Rashidi, P., & Cook, D. J. (2010, December). Mining sensor streams for discovering human activity patterns over time. In *Data Mining (ICDM), 2010 IEEE 10th International Conference on* (pp. 431-440). IEEE.

- [54] Qi, X., Zhou, G., Li, Y., & Peng, G. (2012, December). Radiosense: Exploiting wireless communication patterns for body sensor network activity recognition. In *Real-Time Systems Symposium (RTSS), 2012 IEEE 33rd*(pp. 95-104). IEEE.
- [55] Wang, Y., Liu, J., Chen, Y., Gruteser, M., Yang, J., & Liu, H. (2014, September). E-eyes: device-free location-oriented activity identification using fine-grained wifi signatures. In *Proceedings of the 20th annual international conference on Mobile computing and networking* (pp. 617-628). ACM.
- [56] Kellogg, B., Talla, V., & Gollakota, S. (2014). Bringing gesture recognition to all devices. In *11th USENIX Symposium on Networked Systems Design and Implementation (NSDI 14)* (pp. 303-316).
- [57] Wang, S., & Zhou, G. (2015). A review on radio based activity recognition. *Digital Communications and Networks*, 1(1), 20-29.
- [58] Geng, Y., Chen, J., Fu, R., Bao, G., & Pahlavan, K. (2015). Enlighten wearable physiological monitoring systems: On-body rf characteristics based human motion classification using a support vector machine.
- [59] <http://en.wikipedia.org/wiki/ZigBee>
- [60] Zhou, G., He, T., Krishnamurthy, S., & Stankovic, J. A. (2006). Models and solutions for radio irregularity in wireless sensor networks. *ACM Transactions on Sensor Networks (TOSN)*, 2(2), 221-262.
- [61] Zhou, G., Wan, C. Y., Yarvis, M. D., & Stankovic, J. A. (2007, April). Aggregator-centric QoS for body sensor networks. In *Proceedings of the 6th international conference on Information processing in sensor networks* (pp. 539-540). ACM.
- [62] Zhou, G., Li, Q., Li, J., Wu, Y., Lin, S., Lu, J., ... & Stankovic, J. A. (2011). Adaptive and radio-agnostic qos for body sensor networks. *ACM Transactions on Embedded Computing Systems (TECS)*, 10(4), 48.
- [63] Geng, Y., He, J., & Pahlavan, K. (2013). Modeling the effect of human body on TOA based indoor human tracking. *International Journal of Wireless Information Networks*, 20(4), 306-317.
- [64] He, J., Geng, Y., & Pahlavan, K. (2014). Toward Accurate Human Tracking: Modeling Time-of-Arrival for Wireless Wearable Sensors in Multipath Environment. *Sensors Journal, IEEE*, 14(11), 3996-4006.

- [65] Sigg, S., Blanke, U., & Troster, G. (2014, March). The telepathic phone: Frictionless activity recognition from wifi-rssi. In *Pervasive Computing and Communications (PerCom), 2014 IEEE International Conference on* (pp. 148-155). IEEE.
- [66] Sigg, S., Hock, M., Scholz, M., Troester, G., Wolf, L., Ji, Y., & Beigl, M. (2013). Passive, device-free recognition on your mobile phone: tools, features and a case study. In *Mobile and Ubiquitous Systems: Computing, Networking, and Services* (pp. 435-446). Springer International Publishing.
- [67] Wu, K., Xiao, J., Yi, Y., Gao, M., & Ni, L. M. (2012, March). Fila: Fine-grained indoor localization. In *INFOCOM, 2012 Proceedings IEEE* (pp. 2210-2218). IEEE.
- [68] Adib, F., & Katabi, D. (2013). *See through walls with wifi!* (Vol. 43, No. 4, pp. 75-86). ACM.
- [69] Pu, Q., Gupta, S., Gollakota, S., & Patel, S. (2013, September). Whole-home gesture recognition using wireless signals. In *Proceedings of the 19th annual international conference on Mobile computing & networking* (pp. 27-38). ACM.
- [70] Chen, Z., Wang, S., Chen, Y., Zhao, Z., & Lin, M. (2012, December). InferLoc: calibration free based location inference for temporal and spatial fine-granularity magnitude. In *Computational Science and Engineering (CSE), 2012 IEEE 15th International Conference on* (pp. 453-460). IEEE.
- [71] Wang, Y., Yang, J., Chen, Y., Liu, H., Gruteser, M., & Martin, R. P. (2014, June). Tracking human queues using single-point signal monitoring. In *Proceedings of the 12th annual international conference on Mobile systems, applications, and services* (pp. 42-54). ACM.
- [72] Abdelnasser, H., Youssef, M., & Harras, K. A. (2015, April). Wigest: A ubiquitous wifi-based gesture recognition system. In *Computer Communications (INFOCOM), 2015 IEEE Conference on* (pp. 1472-1480). IEEE.
- [73] Dardas, N. H., & Georganas, N. D. (2011). Real-time hand gesture detection and recognition using bag-of-features and support vector machine techniques. *Instrumentation and Measurement, IEEE Transactions on*, 60(11), 3592-3607.
- [74] Durisi, G., & Benedetto, S. (2003). Performance evaluation of TH-PPM UWB systems in the presence of multiuser interference. *IEEE Communications Letters*, 7(5), 224-226.

- [75] Nanda, S., Balachandran, K., & Kumar, S. (2000). Adaptation techniques in wireless packet data services. *Communications Magazine, IEEE*, 38(1), 54-64.
- [76] Güvenç, İ., Arslan, H., Gezici, S., & Kobayashi, H. (2004, October). Adaptation of multiple access parameters in time hopping UWB cluster based wireless sensor networks. In *Mobile Ad-hoc and Sensor Systems, 2004 IEEE International Conference on* (pp. 235-244). IEEE.
- [77] Perez-Guirao, M. D., Lübben, R., Zhao, Z., Kaiser, T., & Jobmann, K. (2007, September). Cross-Layer MAC Design for IR-UWB Networks. In *Cross Layer Design, 2007. IWCLD'07. International Workshop on* (pp. 113-116). IEEE.
- [78] Fudenberg, D., & Tirole, J. (1991). *Game Theory*, Cambridge and London..
- [79] Movassaghi, S., Abolhasan, M., Lipman, J., Smith, D., & Jamalipour, A. (2014). Wireless body area networks: A survey. *Communications Surveys & Tutorials, IEEE*, 16(3), 1658-1686.
- [80] Poslad, S. (2009). Smart Mobiles, Cards and Device Networks. *Ubiquitous Computing: Smart Devices, Environments and Interactions*, 115-133.
- [81] He, J., Geng, Y., & Pahlavan, K. (2012, September). Modeling indoor TOA ranging error for body mounted sensors. In *Personal Indoor and Mobile Radio Communications (PIMRC), 2012 IEEE 23rd International Symposium on* (pp. 682-686). IEEE.
- [82] http://www.cwins.wpi.edu/publications/Thesis/MS%20Thesis/Guanxiong_Liu_May_2015.pdf
- [83] Pahlavan, K., & Levesque, A. H. (2005). *Wireless information networks* (Vol. 93). John Wiley & Sons.
- [84] Alavi, B., & Pahlavan, K. (2006). Modeling of the TOA-based distance measurement error using UWB indoor radio measurements. *Communications Letters, IEEE*, 10(4), 275-277.
- [85] Zheng, Y., Zang, Y., & Pahlavan, K. (2016, January). UWB localization modeling for electronic gaming. In *2016 IEEE International Conference on Consumer Electronics (ICCE)* (pp. 170-173). IEEE.

Appendix A Original Data

This is the original data of 500 measurements in 6 locations. The data in the table is the distance between the two antennas measurement by the network analyzer using the TOA feature of UWB signal. Using these data, we can calculate the mean and variance of the ranging error.

Table 2 Original data of the distance between the two antennas

location 2		location 3		location 5		location 6		location 8		location 9	
LOS	OLOS	LOS	OLOS	LOS	OLOS	LOS	OLOS	LOS	OLOS	LOS	OLOS
2.735	2.866	2.801	2.502	2.089	2.235	2.358	2.232	2.14	1.944	1.962	1.815
2.707	2.648	2.758	2.487	2.025	2.179	2.313	2.147	2.109	1.928	1.952	1.802
2.708	2.651	2.77	2.488	2.031	2.189	2.319	2.171	2.11	1.931	1.953	1.803
2.708	2.655	2.775	2.495	2.035	2.192	2.319	2.173	2.119	1.933	1.954	1.803
2.708	2.665	2.776	2.502	2.038	2.197	2.32	2.174	2.12	1.933	1.955	1.803
2.709	2.67	2.776	2.51	2.044	2.197	2.32	2.174	2.12	1.933	1.955	1.803
2.711	2.671	2.778	2.513	2.05	2.198	2.321	2.174	2.12	1.933	1.956	1.804
2.711	2.672	2.78	2.525	2.052	2.201	2.321	2.176	2.12	1.933	1.956	1.805
2.712	2.678	2.782	2.454	2.053	2.201	2.322	2.184	2.121	1.934	1.956	1.805
2.712	2.685	2.782	2.455	2.056	2.202	2.322	2.185	2.121	1.934	1.956	1.806
2.712	2.722	2.783	2.456	2.057	2.202	2.322	2.187	2.121	1.934	1.956	1.806
2.712	2.75	2.783	2.458	2.057	2.202	2.323	2.188	2.121	1.934	1.956	1.806
2.713	2.757	2.783	2.458	2.057	2.204	2.323	2.188	2.121	1.934	1.956	1.806
2.713	2.762	2.783	2.464	2.058	2.205	2.324	2.188	2.121	1.934	1.956	1.806
2.713	2.765	2.784	2.464	2.06	2.205	2.324	2.189	2.121	1.934	1.956	1.806
2.713	2.765	2.785	2.465	2.061	2.206	2.324	2.189	2.121	1.935	1.956	1.806
2.713	2.766	2.785	2.466	2.061	2.206	2.325	2.189	2.121	1.935	1.957	1.806
2.714	2.767	2.786	2.467	2.064	2.206	2.325	2.19	2.122	1.935	1.957	1.806
2.715	2.767	2.787	2.467	2.064	2.207	2.325	2.19	2.122	1.935	1.957	1.806
2.715	2.768	2.787	2.468	2.065	2.207	2.325	2.19	2.122	1.935	1.957	1.806
2.715	2.769	2.787	2.468	2.065	2.207	2.325	2.192	2.123	1.935	1.957	1.807
2.715	2.769	2.787	2.47	2.065	2.207	2.325	2.193	2.123	1.935	1.957	1.807
2.716	2.771	2.788	2.471	2.066	2.207	2.325	2.195	2.124	1.935	1.957	1.807
2.716	2.773	2.788	2.472	2.067	2.207	2.325	2.196	2.124	1.935	1.957	1.807

2.716	2.773	2.788	2.472	2.068	2.207	2.326	2.197	2.124	1.936	1.957	1.807
2.716	2.774	2.788	2.472	2.068	2.208	2.326	2.197	2.124	1.936	1.957	1.807
2.717	2.775	2.788	2.472	2.069	2.208	2.326	2.197	2.124	1.936	1.957	1.807
2.717	2.775	2.788	2.473	2.07	2.208	2.326	2.197	2.124	1.936	1.957	1.807
2.717	2.775	2.789	2.473	2.071	2.21	2.326	2.198	2.125	1.936	1.957	1.807
2.717	2.775	2.789	2.474	2.071	2.21	2.327	2.199	2.125	1.936	1.957	1.807
2.717	2.776	2.789	2.474	2.071	2.21	2.327	2.199	2.125	1.936	1.957	1.807
2.717	2.777	2.789	2.474	2.072	2.21	2.327	2.199	2.126	1.936	1.957	1.807
2.718	2.778	2.789	2.475	2.074	2.21	2.328	2.199	2.126	1.937	1.958	1.807
2.718	2.779	2.789	2.475	2.075	2.211	2.328	2.199	2.126	1.937	1.958	1.807
2.718	2.78	2.789	2.475	2.075	2.211	2.328	2.199	2.126	1.937	1.958	1.808
2.718	2.781	2.79	2.476	2.076	2.212	2.328	2.199	2.126	1.937	1.958	1.808
2.718	2.781	2.79	2.477	2.078	2.212	2.328	2.199	2.126	1.937	1.958	1.808
2.718	2.782	2.79	2.478	2.078	2.213	2.328	2.2	2.126	1.937	1.958	1.808
2.718	2.782	2.79	2.478	2.078	2.213	2.328	2.2	2.127	1.937	1.958	1.808
2.718	2.782	2.79	2.478	2.079	2.213	2.328	2.2	2.127	1.937	1.958	1.808
2.718	2.782	2.79	2.478	2.08	2.213	2.329	2.2	2.127	1.937	1.958	1.808
2.719	2.783	2.79	2.479	2.08	2.213	2.329	2.201	2.127	1.937	1.958	1.808
2.719	2.783	2.79	2.479	2.08	2.213	2.329	2.201	2.128	1.937	1.958	1.808
2.719	2.783	2.791	2.479	2.081	2.213	2.329	2.201	2.128	1.937	1.958	1.808
2.719	2.783	2.791	2.479	2.081	2.213	2.329	2.201	2.128	1.937	1.958	1.808
2.719	2.783	2.791	2.479	2.081	2.214	2.329	2.201	2.128	1.937	1.958	1.808
2.719	2.783	2.791	2.48	2.084	2.214	2.329	2.201	2.128	1.937	1.958	1.809
2.719	2.783	2.791	2.48	2.084	2.214	2.329	2.201	2.128	1.937	1.958	1.809
2.72	2.784	2.792	2.48	2.085	2.214	2.329	2.201	2.128	1.937	1.958	1.809
2.72	2.785	2.792	2.48	2.085	2.214	2.329	2.201	2.128	1.937	1.958	1.809
2.72	2.787	2.792	2.48	2.087	2.215	2.33	2.202	2.128	1.937	1.958	1.809
2.72	2.787	2.792	2.481	2.087	2.215	2.33	2.202	2.128	1.937	1.958	1.809
2.72	2.788	2.792	2.481	2.087	2.215	2.33	2.202	2.128	1.937	1.958	1.809
2.72	2.789	2.792	2.481	2.088	2.216	2.33	2.203	2.128	1.937	1.958	1.809
2.72	2.789	2.793	2.481	2.088	2.216	2.33	2.203	2.128	1.938	1.958	1.809
2.721	2.789	2.793	2.482	2.089	2.216	2.331	2.203	2.128	1.938	1.958	1.809
2.721	2.79	2.793	2.482	2.089	2.216	2.331	2.203	2.128	1.938	1.958	1.809
2.721	2.79	2.793	2.483	2.091	2.216	2.331	2.204	2.128	1.938	1.958	1.809
2.721	2.79	2.793	2.483	2.091	2.216	2.331	2.204	2.128	1.938	1.958	1.81
2.721	2.791	2.793	2.483	2.092	2.217	2.331	2.205	2.128	1.938	1.958	1.81
2.721	2.792	2.793	2.483	2.092	2.217	2.331	2.205	2.129	1.938	1.958	1.81
2.721	2.792	2.793	2.483	2.092	2.217	2.332	2.205	2.129	1.938	1.958	1.81
2.722	2.793	2.794	2.484	2.093	2.217	2.332	2.205	2.129	1.938	1.958	1.81

2.722	2.793	2.794	2.484	2.093	2.217	2.332	2.205	2.129	1.938	1.958	1.81
2.722	2.793	2.794	2.484	2.093	2.217	2.332	2.206	2.129	1.938	1.958	1.81
2.722	2.793	2.794	2.484	2.095	2.217	2.332	2.206	2.129	1.938	1.958	1.81
2.722	2.794	2.794	2.484	2.095	2.217	2.333	2.206	2.129	1.938	1.958	1.81
2.722	2.794	2.794	2.484	2.095	2.217	2.333	2.206	2.129	1.938	1.959	1.81
2.722	2.794	2.794	2.484	2.096	2.218	2.333	2.206	2.129	1.938	1.959	1.81
2.722	2.794	2.794	2.485	2.098	2.218	2.333	2.207	2.129	1.938	1.959	1.81
2.722	2.795	2.795	2.485	2.099	2.218	2.334	2.207	2.129	1.938	1.959	1.81
2.722	2.795	2.795	2.485	2.1	2.218	2.334	2.207	2.129	1.938	1.959	1.81
2.722	2.796	2.795	2.485	2.1	2.218	2.334	2.207	2.129	1.938	1.959	1.81
2.723	2.797	2.795	2.485	2.102	2.218	2.334	2.208	2.129	1.938	1.959	1.81
2.723	2.797	2.795	2.485	2.104	2.218	2.335	2.208	2.129	1.938	1.959	1.81
2.723	2.797	2.795	2.485	2.106	2.219	2.335	2.208	2.13	1.938	1.959	1.81
2.723	2.797	2.795	2.485	2.107	2.219	2.335	2.208	2.13	1.938	1.959	1.81
2.723	2.797	2.795	2.485	2.108	2.219	2.335	2.208	2.13	1.938	1.959	1.81
2.723	2.798	2.796	2.486	2.108	2.219	2.335	2.208	2.13	1.939	1.959	1.81
2.723	2.798	2.796	2.487	2.108	2.219	2.335	2.208	2.13	1.939	1.959	1.81
2.723	2.798	2.797	2.487	2.109	2.219	2.335	2.209	2.13	1.939	1.959	1.81
2.723	2.799	2.797	2.487	2.111	2.219	2.336	2.209	2.13	1.939	1.959	1.81
2.723	2.799	2.797	2.487	2.113	2.219	2.336	2.209	2.13	1.939	1.96	1.81
2.724	2.799	2.797	2.487	2.114	2.219	2.337	2.21	2.13	1.939	1.96	1.811
2.724	2.799	2.797	2.488	2.116	2.219	2.337	2.21	2.13	1.939	1.96	1.811
2.724	2.799	2.797	2.488	2.118	2.219	2.337	2.211	2.13	1.939	1.96	1.811
2.724	2.8	2.797	2.488	2.119	2.22	2.337	2.211	2.13	1.939	1.96	1.811
2.724	2.8	2.797	2.488	2.12	2.22	2.337	2.211	2.13	1.939	1.96	1.811
2.724	2.801	2.797	2.488	2.121	2.22	2.337	2.212	2.13	1.939	1.96	1.811
2.724	2.801	2.797	2.488	2.121	2.22	2.337	2.212	2.13	1.939	1.96	1.811
2.724	2.801	2.798	2.488	2.125	2.22	2.338	2.212	2.13	1.939	1.96	1.811
2.724	2.801	2.798	2.488	2.125	2.22	2.339	2.213	2.131	1.939	1.96	1.811
2.724	2.801	2.798	2.488	2.13	2.22	2.339	2.213	2.131	1.939	1.96	1.811
2.724	2.801	2.798	2.488	2.131	2.22	2.34	2.213	2.131	1.939	1.96	1.811
2.725	2.802	2.798	2.488	2.131	2.22	2.342	2.213	2.131	1.939	1.96	1.811
2.725	2.802	2.798	2.488	2.133	2.221	2.346	2.213	2.131	1.939	1.96	1.811
2.725	2.802	2.798	2.488	2.134	2.221	2.346	2.213	2.131	1.939	1.96	1.811
2.725	2.802	2.798	2.489	2.136	2.221	2.348	2.214	2.131	1.939	1.96	1.811
2.725	2.802	2.798	2.489	2.136	2.221	2.349	2.214	2.131	1.939	1.96	1.811
2.725	2.803	2.798	2.489	2.139	2.221	2.349	2.214	2.131	1.939	1.96	1.811
2.725	2.803	2.799	2.489	2.146	2.221	2.349	2.214	2.131	1.939	1.96	1.811
2.725	2.803	2.799	2.489	2.154	2.221	2.349	2.214	2.132	1.939	1.96	1.811

2.742	2.884		2.513	2.092	2.253	2.37	2.182	2.146	1.947	1.964	1.818
2.742	2.885		2.513	2.092	2.254	2.37	2.19	2.146	1.947	1.964	1.818
2.742	2.885		2.513	2.092	2.254	2.37	2.19	2.146	1.947	1.964	1.818
2.742	2.885		2.513	2.092	2.256	2.37	2.19	2.146	1.947	1.964	1.818
2.742	2.885		2.513	2.092	2.256	2.37	2.19	2.146	1.947	1.964	1.818
2.743	2.887		2.513	2.092	2.256	2.37	2.194	2.146	1.947	1.964	1.818
2.743	2.887		2.513	2.092	2.256	2.37	2.195	2.146	1.947	1.964	1.818
2.743	2.888		2.513	2.092	2.257	2.37	2.201	2.146	1.947	1.964	1.819
2.743	2.888		2.513	2.093	2.257	2.37	2.202	2.146	1.947	1.964	1.819
2.743	2.889		2.514	2.093	2.257	2.37	2.203	2.146	1.948	1.964	1.819
2.743	2.89		2.514	2.093	2.257	2.37	2.204	2.147	1.948	1.964	1.819
2.743	2.89		2.514	2.093	2.257	2.37	2.205	2.147	1.948	1.964	1.819
2.743	2.89		2.514	2.093	2.258	2.37	2.207	2.147	1.948	1.964	1.819
2.743	2.89		2.515	2.093	2.258	2.37	2.207	2.147	1.948	1.964	1.819
2.743	2.892		2.515	2.093	2.258	2.37	2.208	2.147	1.948	1.964	1.819
2.744	2.892		2.515	2.093	2.258	2.37	2.208	2.147	1.948	1.964	1.819
2.744	2.892		2.515	2.093	2.259	2.37	2.21	2.147	1.948	1.964	1.819
2.744	2.892		2.515	2.093	2.26	2.37	2.213	2.147	1.948	1.964	1.819
2.744	2.893		2.515	2.093	2.26	2.37	2.213	2.147	1.948	1.964	1.819
2.744	2.893		2.515	2.093	2.261	2.37	2.213	2.147	1.948	1.964	1.819
2.744	2.894		2.515	2.093	2.261	2.371	2.215	2.147	1.948	1.964	1.819
2.744	2.895		2.515	2.093	2.263	2.371	2.217	2.147	1.948	1.964	1.819
2.744	2.895		2.515	2.093	2.263	2.371	2.217	2.147	1.948	1.964	1.819
2.745	2.895		2.515	2.093	2.263	2.371	2.217	2.147	1.948	1.964	1.819
2.745	2.895		2.516	2.093	2.263	2.371	2.218	2.147	1.948	1.964	1.819
2.745	2.896		2.516	2.093	2.265	2.371	2.218	2.147	1.948	1.964	1.819
2.745	2.897		2.516	2.093	2.265	2.371	2.218	2.147	1.948	1.964	1.819
2.745	2.898		2.516	2.093	2.267	2.371	2.218	2.147	1.948	1.964	1.819
2.745	2.899		2.516	2.093	2.268	2.371	2.22	2.147	1.948	1.964	1.819
2.745	2.899		2.516	2.093	2.269	2.371	2.22	2.148	1.948	1.964	1.819
2.745	2.9		2.516	2.093	2.269	2.371	2.221	2.148	1.948	1.964	1.819
2.745	2.901		2.516	2.094	2.271	2.371	2.221	2.148	1.948	1.964	1.819
2.745	2.901		2.517	2.094	2.271	2.371	2.221	2.148	1.949	1.964	1.819
2.745	2.901		2.517	2.094	2.274	2.371	2.222	2.148	1.949	1.964	1.819
2.746	2.901		2.517	2.094	2.274	2.371	2.222	2.148	1.949	1.964	1.819
2.746	2.902		2.517	2.094	2.279	2.371	2.223	2.148	1.949	1.964	1.819
2.746	2.903		2.517	2.094	2.282	2.371	2.225	2.148	1.949	1.965	1.82
2.746	2.903		2.517	2.094	2.287	2.371	2.225	2.148	1.949	1.965	1.82
2.746	2.904		2.517	2.094	2.289	2.371	2.225	2.148	1.949	1.965	1.82

2.746	2.906		2.517	2.094	2.292	2.371	2.225	2.148	1.949	1.965	1.82
2.746	2.906		2.517	2.094	2.306	2.371	2.225	2.148	1.949	1.965	1.82
2.747	2.907		2.517	2.094	2.326	2.371	2.226	2.148	1.949	1.965	1.82
2.747	2.91		2.517	2.094	2.123	2.371	2.229	2.148	1.949	1.965	1.82
2.747	2.91		2.517	2.094	2.156	2.372	2.229	2.148	1.949	1.965	1.82
2.747	2.91		2.517	2.094	2.172	2.372	2.229	2.148	1.949	1.965	1.82
2.747	2.91		2.517	2.094	2.186	2.372	2.229	2.148	1.949	1.965	1.82
2.747	2.91		2.518	2.094	2.186	2.372	2.229	2.148	1.949	1.965	1.82
2.747	2.91		2.518	2.094	2.191	2.372	2.23	2.148	1.949	1.965	1.82
2.747	2.911		2.518	2.094	2.199	2.372	2.23	2.148	1.949	1.965	1.82
2.747	2.912		2.518	2.094	2.203	2.372	2.23	2.149	1.949	1.965	1.82
2.748	2.912		2.519	2.094	2.212	2.372	2.231	2.149	1.949	1.965	1.82
2.748	2.912		2.519	2.094	2.212	2.372	2.231	2.149	1.949	1.965	1.82
2.748	2.913		2.519	2.094	2.216	2.372	2.231	2.149	1.949	1.965	1.82
2.748	2.913		2.519	2.095	2.218	2.372	2.231	2.149	1.949	1.965	1.82
2.748	2.913		2.519	2.095	2.22	2.372	2.232	2.149	1.949	1.965	1.821
2.748	2.913		2.519	2.095	2.222	2.372	2.232	2.149	1.949	1.965	1.821
2.748	2.914		2.519	2.095	2.224	2.373	2.232	2.149	1.949	1.965	1.821
2.748	2.914		2.519	2.095	2.225	2.373	2.233	2.149	1.949	1.965	1.821
2.748	2.914		2.519	2.095	2.225	2.373	2.234	2.149	1.949	1.965	1.821
2.748	2.916		2.519	2.095	2.231	2.373	2.234	2.149	1.949	1.965	1.821
2.748	2.917		2.519	2.095	2.234	2.374	2.235	2.149	1.95	1.965	1.821
2.748	2.919		2.519	2.095	2.234	2.374	2.235	2.149	1.95	1.965	1.821
2.748	2.919		2.519	2.095	2.235	2.374	2.236	2.149	1.95	1.965	1.821
2.748	2.919		2.519	2.096	2.236	2.374	2.236	2.149	1.95	1.965	1.821
2.749	2.921		2.52	2.096	2.238	2.374	2.236	2.149	1.95	1.965	1.821
2.749	2.922		2.52	2.096	2.239	2.374	2.236	2.149	1.95	1.965	1.821
2.749	2.923		2.52	2.096	2.239	2.374	2.236	2.15	1.95	1.965	1.821
2.749	2.924		2.52	2.096	2.241	2.374	2.236	2.15	1.95	1.965	1.821
2.749	2.924		2.52	2.096	2.241	2.374	2.238	2.15	1.95	1.965	1.821
2.749	2.925		2.52	2.096	2.242	2.374	2.238	2.15	1.95	1.965	1.821
2.749	2.925		2.52	2.096	2.242	2.374	2.238	2.151	1.95	1.965	1.821
2.75	2.925		2.52	2.096	2.243	2.374	2.239	2.151	1.95	1.965	1.821
2.75	2.926		2.52	2.096	2.244	2.374	2.239	2.151	1.951	1.965	1.821
2.75	2.926		2.52	2.096	2.244	2.374	2.239	2.151	1.951	1.965	1.821
2.75	2.928		2.52	2.096	2.246	2.374	2.24	2.151	1.951	1.965	1.821
2.751	2.929		2.52	2.096	2.247	2.374	2.241	2.151	1.951	1.965	1.821
2.751	2.931		2.52	2.096	2.248	2.374	2.241	2.151	1.951	1.965	1.821
2.751	2.934		2.52	2.097	2.248	2.374	2.242	2.151	1.951	1.965	1.821

2.751	2.934		2.52	2.097	2.248	2.374	2.242	2.151	1.951	1.965	1.821
2.751	2.937		2.521	2.097	2.249	2.374	2.243	2.151	1.951	1.965	1.822
2.751	2.938		2.521	2.097	2.249	2.374	2.243	2.151	1.951	1.965	1.822
2.751	2.945		2.521	2.097	2.252	2.375	2.243	2.151	1.951	1.965	1.822
2.751	2.945		2.521	2.097	2.252	2.375	2.243	2.152	1.951	1.965	1.822
2.751	2.946		2.521	2.097	2.252	2.375	2.244	2.152	1.951	1.965	1.822
2.751	2.949		2.522	2.097	2.253	2.375	2.245	2.152	1.951	1.965	1.822
2.752	2.953		2.522	2.097	2.253	2.375	2.245	2.152	1.951	1.965	1.822
2.752	2.953		2.522	2.097	2.254	2.375	2.246	2.152	1.951	1.965	1.822
2.752	2.955		2.522	2.098	2.255	2.375	2.246	2.152	1.951	1.965	1.822
2.752	2.955		2.522	2.098	2.256	2.375	2.246	2.152	1.951	1.965	1.822
2.752	2.956		2.522	2.098	2.256	2.375	2.247	2.152	1.951	1.965	1.822
2.752	2.962		2.523	2.098	2.257	2.375	2.248	2.152	1.952	1.965	1.822
2.752	2.962		2.523	2.098	2.257	2.375	2.248	2.153	1.952	1.965	1.822
2.753	2.963		2.523	2.098	2.257	2.375	2.248	2.153	1.952	1.965	1.822
2.753	2.967		2.524	2.098	2.257	2.375	2.249	2.153	1.952	1.965	1.822
2.753	2.969		2.524	2.098	2.257	2.375	2.249	2.153	1.952	1.965	1.822
2.753	2.979		2.524	2.098	2.258	2.375	2.25	2.153	1.952	1.965	1.822
2.754	2.983		2.524	2.098	2.258	2.375	2.252	2.153	1.952	1.966	1.822
2.754	2.985		2.525	2.098	2.259	2.375	2.252	2.153	1.952	1.966	1.822
2.754	3.124		2.525	2.098	2.259	2.376	2.252	2.153	1.952	1.966	1.823
2.754	3.137		2.525	2.098	2.26	2.376	2.253	2.153	1.952	1.966	1.823
2.754	3.139		2.525	2.098	2.26	2.376	2.253	2.154	1.952	1.966	1.823
2.754	3.143		2.525	2.099	2.261	2.376	2.253	2.154	1.953	1.966	1.823
2.754	3.152		2.525	2.099	2.261	2.376	2.254	2.154	1.953	1.966	1.824
2.754	3.158		2.526	2.099	2.263	2.376	2.255	2.154	1.953	1.966	1.824
2.755	3.163		2.526	2.099	2.263	2.376	2.256	2.154	1.953	1.966	1.824
2.756	3.169		2.527	2.099	2.267	2.376	2.256	2.154	1.953	1.966	1.824
2.756	3.183		2.527	2.099	2.271	2.376	2.257	2.154	1.953	1.966	1.824
2.756	3.189		2.528	2.1	2.277	2.378	2.258	2.155	1.953	1.966	1.824
2.756	3.19		2.528	2.1	2.286	2.378	2.258	2.155	1.953	1.966	1.824
2.757	3.196		2.528	2.1	2.29	2.378	2.259	2.155	1.954	1.966	1.824
2.758	3.214		2.53	2.101	2.293	2.378	2.261	2.156	1.954	1.966	1.824
2.758	3.221		2.531	2.101	2.294	2.379	2.261	2.156	1.954	1.966	1.824
2.758	3.227		2.531	2.101	2.296	2.379	2.261	2.156	1.954	1.966	1.824
2.758	3.253		2.531	2.102	2.3	2.379	2.262	2.156	1.954	1.966	1.824
2.76	3.256		2.532	2.102	2.31	2.379	2.262	2.156	1.954	1.967	1.825
2.761	3.265		2.532	2.102		2.379	2.263	2.156	1.954	1.967	1.825
2.761	3.28		2.534	2.102		2.38	2.264	2.157	1.954	1.967	1.825

2.761	3.288		2.535	2.102		2.38	2.265	2.157	1.955	1.967	1.825
2.762	3.298		2.535	2.102		2.381	2.265	2.158	1.955	1.967	1.825
2.762	3.302		2.535	2.102		2.381	2.266	2.158	1.955	1.967	1.825
2.766	3.316		2.536	2.103		2.381	2.267	2.158	1.955	1.967	1.826
2.766	3.335		2.536	2.103		2.382	2.268	2.16	1.956	1.967	1.826
2.766	3.386		2.538	2.103		2.383	2.275	2.16	1.956	1.967	1.827
2.767	3.415		2.54	2.103		2.383	2.276	2.16	1.956	1.967	1.828
2.77	3.552		2.54	2.106		2.385	2.28	2.165	1.956	1.967	1.829
2.802	3.56		2.54	2.108		2.391	2.285	2.173	1.956	1.968	1.829

Appendix B Core code

Data collection:

```
%% Automate Placetool
```

```
%% Placetool should be running and the floormap should be loaded first!
```

```
clear all
```

```
close all
```

```
clc
```

```
filenumber = input('Point number: ');
```

```
    if filenumber == -1
```

```
        break
```

```
    end
```

```
for num=1:filenumber
```

```
    filename1 = ['F:\scen3_pt' num2str(num)];
```

```
    % filename2 = ['scen3_pt' num2str(num) '_2'];
```

```
    dos(['"D:\Program Files\AutoHotkey\Autohotkey.exe" vic.ahk ' filename1 ' ']);
```

```
end
```

```
% Compute Channel Impulse Response from frequency measurement
```

```
% data using Chirp-Z transform with hanning window.
```

```
% modified 03/27/02.
```

```
function [ zt_han , t ] = czt_hanning(freq, Zf, tstart, tstop, flag, Nt )
```

```

%Nf = length(freq);
Nf = length(freq);
df = (freq(Nf)-freq(1))/(Nf-1);

T = 1/df;

if nargin < 6
    % Nt = 1601;
    Nt = 1601;
end;

if flag == 1
    han = hanning(Nf);
%   han = hann(Nt);
    Zf = (45/23)*Zf(:).*han(:); % 45/23 is to make the Hanning-window time response peak at
1.
%   Zf = Zf(:).*han(:);
end;

dt = (tstop-tstart)/(Nt-1);
w = exp(1j*2*pi*dt/T);
a = exp(1j*2*pi*tstart/T);

zt_han = (1/Nf)*czt(Zf(:), Nt, w, a);

t = linspace(tstart, tstop, Nt);

return;

```

```

%
% This program is used to load 8753D Network Analyzer Measurement data.
% Read S21 data from S1P file.  LogMag/Angle.
%

```

```

function [ Hf, f ] = load_chmeas_s1p_dB( fname, flag_fig)

```

```

%fid = fopen(fname, 'rt');

```

```

fid = fopen(fname, 'rt');

```

```

if fid == -1

```

```

    disp(['File cannot be opened !']);

```

```

    Hf = 0;  f = 0;

```

```

    return;

```

```

end;

```

```

while( 1 )

```

```

    temp_str = fgetl(fid);  % read in a line of text.

```

```

    if temp_str(1) == '!'

```

```

        if flag_fig == 1

```

```

            disp(temp_str);

```

```

        end;

```

```

    else

```

```

        if temp_str(1) == '#'

```

```

            tmp_data = fscanf(fid, '%g %g %g', [3 inf] );

```

```

            fclose(fid);

```

```

            tmp_data = tmp_data.';

```

```

            f = tmp_data(:,1);

```

```

            amp = 10.^(tmp_data(:,2)/20);

```

```

            % Channel Transfer Function measured by VNA

```

```

        %      Hf = 10.^(tmp_data(:,2)/20).*exp(1j*tmp_data(:,3)*pi/180);
        Hf = amp.*exp(1j*tmp_data(:,3)*pi/180);
        break;
    else
        if feof(fid)
            fclose(fid);
            Hf = 0;  f = 0;
            return;
        end;
    end;
end;
end;
end;

% %Plot figure in frequency domain - disable while looping
% if flag_fig == 1
%     tmp_f = f*1e-9;
%     mag_dB = 10*log10(abs(Hf));
%     phs = angle(Hf.);
%
%     figure; hold on; box on;
%     subplot(2,1,1); plot(tmp_f, mag_dB);
%     subplot(2,1,1); plot(tmp_f, mag_dB);
%     xlabel('frequency (GHz)');
%     ylabel('Magnitude (dB)');
%     title(fname);
%
%     subplot(2,1,2); plot(tmp_f, phs);
%     xlabel('frequency (GHz)');
%     ylabel('angle (radian)');
% end;

```

```

return;

clear all
clc

OrgBand=5e9; %Original Bandwidth from 3Ghz to 8Ghz

B_start=3e9; %Low frequency of select Bandwidth

Band=0.5e9; %Slected Bandwidth

noi = -100; %noise threshold
side =-25;

tstart=0e-9;
if Band>0.3e9
    tstop = 30e-9;
else
    tstop = 100e-9;
end

% n_tstart=200e-9;
% n_tstop=300e-9;

secPeak=1.62*10^(-9);
peak_width=1;
flag_fig = 1;
ampResult = [];

```



```

delayResult = [];
index = [];
ftoa=[];
ftoa_delay=[   ];
ftoa_amp=[   ];

TOA_dis=[   ];

firstPeakDelay = [   ];
firstPeakAmp = [   ];

strange = [ ];
record = [ ];

P_num=fix((Band/OrgBand)*1601);
if B_start~=3e9
    P_start=fix(((B_start-3e9)/OrgBand)*1601);
else
    P_start=1;
end

P_stop=P_start+P_num-1;

WaveLength= 3e8/Band;

RSS=[];
PK=[];
PKgain=[];
PKdis=[];
noise_PKgain=[];

```

```

noise_PKgain_1=[];

maxPKgain=[];

DDP=[];
NDDP=[];
UDP=[];
DDP_num=0;
NDDP_num=0;
UDP_num=0;

Fig=1;
number=235;
bias=14;
% Profile_number=min(10,number);

noise_thred = -100;    %noise threshold
side =-50;

if Fig==1
    figure(5);hold on;grid on;
    xlabel('Delay (s)');
    ylabel('Path Loss (mV)');
    title('Time Domain');
end

for j=1:number
    strange(1,j)=j;

```

```

        fname = ['scen3_pt' num2str(strange(1,j)) '.s1p'];
        Profile_number=min(10,number);
%           [Hf1, f1] = load_chmeas_s1p_dB( fname, flag_fig );
for i=1:1

%   fname = ['scen3_pt2.s1p'];
%
%   [Hf1, f1] = load_chmeas_s1p_dB( fname, flag_fig );

%%%%%%%%%%%%%%%%%%%%%%%%%%%%%%%%%%%%%%%%%%%%%%%%%%%%%%%%%%%%%%%%%%%%%%%%Jie He(db)find RSS %%%%%%%%%%%%%%%

fid = fopen(fname, 'rt');

if fid == -1
    disp(['File cannot be opened !']);
    Hf = 0;   f = 0;
    return;
end;

while( 1 )
    temp_str = fgetl(fid);   % read in a line of text.

    if temp_str(1) == '!'
        if flag_fig == 1
            disp(temp_str);
        end;
    else
        if temp_str(1) == '#'
            tmp_data = fscanf(fid, '%g %g %g', [3 inf] );
            fclose(fid);

```

```

    tmp_data = tmp_data.';
    f = tmp_data(:,1);
    amp = 10.^(tmp_data(:,2)/20);
    % Channel Transfer Function measured by VNA
    %      Hf = 10.^(tmp_data(:,2)/20).*exp(1j*tmp_data(:,3)*pi/180);
    Hf = amp.*exp(1j*tmp_data(:,3)*pi/180);
    break;
else
    if feof(fid)
        fclose(fid);
        Hf = 0;  f = 0;
        return;
    end;
end;
end;
end;

f_dB=20*log10(abs(amp))-bias;
RSS_dB=mean(f_dB);

RSS=[RSS,RSS_dB];

%%%%%%%%%%%%%%%%%%%%%%%%%%%%%%%%%%%%%%%%%%%%%%%%%%%%%%%%%%%%%%%%%%%%%%%%Jie He(db)find RSS %%%%%%%%%%%%%%%

% [zt_han, t] = czt_hanning( f1, Hf1, tstart, tstop, 1, 1601*1000);

% [zt_han, t] = czt_hanning( f1, Hf1, tstart, tstop, 1, 1601);

Hf=Hf(P_start:P_stop);

```

```

f=f(P_start:P_stop);
[zt_han, t] = czt_hanning( f, Hf, tstart, tstop, 1, 1601*10);

time_dB = 20*log10(abs(zt_han))-bias;

%%%%%%%%%%%%%%%%%%%%%%%%%%%%%%%%%%%%%%%%%%%%%%%%%%%%%%%%%%%%%%%%%%%%%%%%Jie He(db)find noise %%%%%%%%%%%%%%%

% Num_start=fix((n_tstart/tstop)*length(t));
% Num_stop=fix((n_tstop/tstop)*length(t));
%
%
%
% noise_index = pkd_cir(time_dB( Num_start:Num_stop), noise_thred, side,
peak_width)+Num_start;
%
% if length(noise_index)~=0
%     noise_PKgain_1=[];
%     for k=1:length(noise_index)
%         noise_PKgain_1=[noise_PKgain_1,20*log10(abs(zt_han(noise_index(k))))-bias];
%         noise_PKgain=[noise_PKgain, 20*log10(abs(zt_han(noise_index(k))))-bias];
%     end
% end

%%%%%%%%%%%%%%%%%%%%%%%%%%%%%%%%%%%%%%%%%%%%%%%%%%%%%%%%%%%%%%%%%%%%%%%%Jie He(db)find noise %%%%%%%%%%%%%%%

%%%%%%%%%%%%%%%%%%%%%%%%%%%%%%%%%%%%%%%%%%%%%%%%%%%%%%%%%%%%%%%%%%%%%%%%Jie He(db) finde peak %%%%%%%%%%%%%%%

```

```

index = pkd_cir(time_dB, noi, side, peak_width);

%%%%%%%%%%%%%%%%%%%%%%%%%%%%%%%%%%%%%%%%%%%%%%%%%%%%%%%%%%%%%%%%%%%%%%%%original(mw)%%%%%%%%%%%%%%%%%%%%%%%%%%%%%%%%%%%%%%%%%%%%%%%%%%%%%%%%%%%%%%%%%%%%%%%%
% index = pkd_cir(abs(zt_han), noi, side, peak_width);
if index == 0
    continue
end

ftoa_delay = [ftoa_delay t(index(1))];
ftoa_amp = [ftoa_amp 20*log10(abs(zt_han(index(1))))-bias];

% Plot Time Response in Time Domain - disable for looping

% if Fig==1 && Profile_number~=0
% %     figure(5);hold on;grid on;
% %     plot(t,time_dB,'b');
%     figure(5);hold on;grid on;
%     plot(t(index(1:length(index))),20*log10(abs(zt_han(index(1:length(index)))))-bias,'bo');
%     plot(ftoa_delay,ftoa_amp,'ro');
% %
% %     if length(noise_index)~=0
% %         plot(t(noise_index),noise_PKgain_1,'bo');
% %     end
%
%     Profile_number=Profile_number-1;
% end

```

```

for k=1:length(index)
    PKgain(i,k)= 20*log10(abs(zt_han(index(k))))-bias;
    PKdis(i,k)=t(index(k))*2.99792458*10^8;

    PK(i,2*(k-1)+2) = 20*log10(abs(zt_han(index(k))))-bias;
    PK(i,2*(k-1)+1)=t(index(k))*2.99792458*10^8;
end

maxPKgain(i)=max(PKgain(i,1:k));

if PKdis(i,1)>=5.059-3e8/Band && PKdis(i,1)<=5.059+3e8/Band
    if PKgain(i,1)==maxPKgain(i);
        DDP=[DDP i];
        DDP_num=DDP_num+1;
    else
        NDDP=[NDDP i];
        NDDP_num=NDDP_num+1;
    end
else
    UDP=[UDP i];
    UDP_num=UDP_num+1;
end

```

```

% for k=1:length(index)
% ftoa(k)= min(t(index(k)));
% gain = abs(zt_han(index(k)));
% power=10*log10(sum(gain.*gain));s

```

```

% end
%
% for ii=1:length(index)
%     pk_gain = abs(zt_han(index(ii)));
%     pk_delay = t(index(ii));
%     fprintf(Rfid,'%g                %g\n\n',pk_gain,pk_delay);
% end

```

```
end
```

```
ftoa_dist=ftoa_delay*2.99792458*10^8;
```

```
TOA_dis=sort(ftoa_dist);
```

```
TOA_Error=TOA_dis-5.059;
```

```
Mean_RSS=mean(RSS)
```

```
Mean_FP=mean(ftoa_amp)
```

```
Mean_dis=mean(TOA_dis)
```

```
Var_RSS=var(RSS)
```

```
Var_FP=var(ftoa_amp)
```

```
Var_dis=var(TOA_dis)
```

```
% if length(noise_PKgain)~=0
```

```
%     Mean_Noise=mean(noise_PKgain)
```

```
% end
```

```
% Max_Noise=max(noise_PKgain);
```



```

% figure(4);hold on;grid on;
% title(' First Path Path Loss versus TOA distance');
% xlabel('TOA distance (m)');
% ylabel('Path Loss (dB)');
%
% ftoa_dist=ftoa_delay*2.99792458*10^8;
% figure(4);hold on;
% plot(ftoa_dist,ftoa_amp,'*');

% m=1:1:length(ftoa_dist);
%
% figure(3); hold on; grid on;
% title('TOA distance in sequence');
% xlabel('Sequence');
% ylabel('TOA distance(m)');
% plot(m,ftoa_dist,'*-');

% strange=[];
% sm=0;
% for i=1:length(ftoa_dist)
%
%     if ftoa_dist(i)<5.059
%         sm=sm+1;
%         strange(1,sm)= i;
%         strange(2,sm)=ftoa_dist(i);
%     end

```

```

% end
%
% BS=int2str(Band/(1e6));
%
% fname = [BS 'MHz'];
% save(fname);
%
% if(sm > 0)
%     figure(4);hold on;grid on;
%     xlabel('Delay (s)');
%     ylabel('Path Loss (dB)');
%     title('Time Domain');
%     for i=1:sm
%         fname = ['scen3_pt' num2str(strange(1,i)) 's1p'];
%         [Hf1, f1] = load_chmeas_s1p_dB( fname, flag_fig );
%         [zt_han, t] = czt_hanning( f1, Hf1, tstart, tstop, 1, 1601);
%         time_dB = 20*log10(abs(zt_han))-bias;
%         figure(4);hold on;grid on;
%         plot(t,time_dB);
%         figure(4);hold on;grid on;
%     title(' First Path Path Loss versus TOA distance');
%     xlabel('TOA distance (m)');
%     ylabel('Path Loss (dB)');
%
%     ftoa_dist=ftoa_delay*2.99792458*10^8;
%     figure(4);hold on;
%     plot(ftoa_dist,ftoa_amp,'*');
%
%         %%%%%%%%%%%%%%%Jie He(db)%%%%%%%%%%%%%%
%
%     index = pkd_cir(time_dB, noi, side, peak_width);

```

```

%
%         if index == 0
%             continue
%         end
%
%
%         figure(6);hold on;grid on;
%
plot(t(index(1:length(index))),20*log10(abs(zt_han(index(1:length(index))))))-bias,'bo');
%         plot( t(index(1)),20*log10(abs(zt_han(index(1)))))-bias,'ro');
%     end
% end
figure(6);hold on;grid on;
    plot(t,10.^(time_dB./20),'b');

    end

m=1:1:length(ftoa_dist);
figure(3); hold on; grid on;
title('TOA distance in sequence');
xlabel('Sequence');
ylabel('TOA distance(m)');
plot(m,ftoa_dist,'*-');
%
    figure(4);hold on;grid on;
title(' First Path Path Loss versus TOA distance');
xlabel('TOA distance (m)');
ylabel('Path Loss (dB)');

% ftoa_dist=ftoa_delay*2.99792458*10^8;
% figure(4);hold on;

```

```

% plot(ftoa_dist,ftoa_amp,'*');
for j = 1: number;
    record(j,1) = ftoa_dist(1,j);
end

% for k=1:length(index)
% ftoa(k)= min(t(index(k)));
% gain = abs(zt_han(index(k)));
% power=10*log10(sum(gain.*gain));
% end

% for ii=1:length(index)
%     pk_gain = abs(zt_han(index(ii)));
%     pk_delay = t(index(ii));
%     fprintf(Rfid,'%e                %e\n\n',pk_gain,pk_delay);
% end
% fclose(Rfid);

% Separate Tap Amplitude and Delay
% Sfid = fopen('Result.txt','r');
% tResult = fscanf(Sfid,'%g');
% for tNum = 1:length(tResult)
%     test = tResult(tNum);
%     if mod(tNum,2)==0
%         delayResult = [delayResult test];           % Save Delay info to Matrix
delayResult[]
%     else ampResult = [ampResult test];           % Save Amplitude info to Matrix
ampResult[]
%     end

```

```

% end

% fclose(Rfid);

% for tPeak=1:length(delayResult)
%     if(delayResult(tPeak)>=0 && delayResult(tPeak)<=secPeak)
%         firstPeakDelay = [firstPeakDelay delayResult(tPeak)];
%         firstPeakAmp = [firstPeakAmp ampResult(tPeak)];
%     end
% end

% figure(1); hold on;grid on;
% Amp_dB = 20*log10(abs(ampResult));
% % plot(delayResult,Amp_dB,'*');
% title('Path Amplitude variance versus Path Delay With Water in Phantom');
% xlabel('Path Delay (ns)');
% ylabel('Path Ampiltude (dB)');
% %axis([1.1e-9 1.6e-9 -80 -35]);

% actDist=0.2286; % thickness of phantom 0.2286m
% figure(3);hold on;grid on;
% firstPeakAmp_dB = 20*log10(abs(firstPeakAmp));
% firstPeakDist = firstPeakDelay*3*(10^9)-actDist;
% plot(firstPeakDist,firstPeakAmp_dB,'*');
% title(' Distance Measurement Error versus Path Delay With Water in Phantom');
% xlabel('Path Delay (m)');
% ylabel('Path Ampiltude (dB)');
% axis([1.35e-9 1.4e-9 -80 -65]);

```

```

% ftoa_dist=ftoa_delay*3*10^8;

% Peak detection on channel impulse response.
%
% input:
%     ht: channel impulse response
%     noi: threshold for noise std
%     side: sidelobe amplitude for window functions
%           Rec: -13dB, Hanning: -32dB, Hamming: -43dB
%     peak_width: time resolution of peak in units of dt

function [ peak_index ] = pkd_cir(ht, noi, side, peak_width)
% peak_width is not used in this version.

len_t = length(ht);
peak = max(ht);

peak_index = 0;
count = 0;
i = 2;
while(1)
    %%%%%%%%%%%%%%%Original(mw)%%%%%%%%%%%%%%
%     if ht(i)>ht(i-1) & ht(i)>ht(i+1) & ht(i)>noi & ht(i)/peak > side
    %%%%%%%%%%%%%%%Original%%%%%%%%%%%%%%
    %%%%%%%%%%%%%%%Jie He(db)%%%%%%%%%%%%%%
    if ht(i)>ht(i-1) & ht(i)>ht(i+1) & ht(i)>noi & ht(i)-peak > side
        %%%%%%%%%%%%%%%Jie He%%%%%%%%%%%%%%
        if ht(i) == peak
            a = i;
        end;
    end;
end;

```

```

        if count == 0
            peak_index = i;
            count = 1;
        else
            peak_index = [peak_index, i];
        end;
        i = i + 1;
    else
        i = i + 1;
    end;

    if i > len_t - 1
        break;
    end;
end;

return;

```

Data analysis:

```

%%%Data Analysis for PNA%%%
clear all;
clc;
data = xlsread('Book9-1.xlsx');
oridata = data;
data = abs(data);
datasort = sort(data);
length_data = size(datasort);
scale = 1/length_data(1,1);

y=[];
y(1,1)=1*scale;

```

```

for i=1:length_data(1,1)-1;
y(i+1,1)=y(i,1)+1*scale;
end
figure(1)
plot(datasort,y, 'linewidth', 1.5);
ylim([0,1]);hold on;
title('Cumulative Distribution Function of Error');
xlabel('Error in meter');
ylabel('Probability');
grid on;box on;

```

```

figure(2)
oridatamin=min(oridata);
oridatamax=max(oridata);
x1=linspace(oridatamin,oridatamax,100);
yy1=hist(oridata,x1);
plot(x1,yy1*scale*100,'linewidth', 2);
xlabel('Error in meter');
ylabel('Probability %');
hold on;grid on;

```

```

figure(3)
x2=linspace(oridatamin,oridatamax,100)- 0.004445;
yy=hist(oridata,x2);
yy=yy/length(oridata);
bar(x2,yy*100);
xlabel('Error in meter');
ylabel('Probability %');
title('Probability Distribution Function of Error');
hold on;grid on;

```